For Reference

NOT TO BE TAKEN FROM THIS ROOM

For Reference

NOT TO BE TAKEN FROM THIS ROOM

Ex libris
universitatis
albertaensis

University of Alberta
Printing Department

Digitized by the Internet Archive
in 2018 with funding from
University of Alberta Libraries

https://archive.org/details/gashydratesystem00ldso

Thesis
1962
#41

THE UNIVERSITY OF ALBERTA

THE GAS HYDRATE SYSTEMS OF SULFUR HEXAFLUORIDE AND SULFUR HEXAFLUORIDE-METHANE

A THESIS
SUBMITTED TO THE FACULTY OF GRADUATE STUDIES
IN PARTIAL FULFILMENT OF THE REQUIREMENTS FOR THE DEGREE
OF MASTER OF SCIENCE IN CHEMICAL ENGINEERING

DEPARTMENT OF CHEMICAL AND PETROLEUM ENGINEERING

by

L.D. SORTLAND

EDMONTON, ALBERTA

JANUARY 9, 1962

ABSTRACT

The molecular structure of gas hydrates has been investigated by previous workers using X-ray diffraction techniques and, based on these results and on statistical mechanics, other investigators have proposed a theory describing the gas hydrate crystal structure. It was the purpose of this investigation to test this theory and to apply it to hydrates containing sulfur hexafluoride.

The pressure-temperature phase equilibrium diagram was experimentally determined for the gas hydrate of sulfur hexafluoride from -8.14 to 12.84°C. From this diagram the composition of the hydrate was determined to be 17.02 ± 0.1 moles of water per mole of sulfur hexafluoride in the hydrate at 0°C. At this temperature the difference between the chemical potential of the water in the "empty" hydrate lattice of Structure II and in the ordinary states was calculated from experimental data to be 211 calories per gram mole of water and from a semi-theoretical method to be 192 calories per gram mole of water.

The pressure-composition phase diagram was experimentally determined on a water-free basis for the sulfur hexafluoride-methane hydrate at -3°C. The experimental phase diagram and the diagram predicted from statistical mechanical theory showed close agreement over most of the pressure range investigated.

Equilibrium constants for sulfur hexafluoride and methane were calculated from the pressure-composition phase diagram for the sulfur hexafluoride-methane hydrate at -3°C. Comparison of these equilibrium constants for methane with those which have been reported by other authors show poor agreement.

ACKNOWLEDGEMENTS

Sincere thanks are extended to Dr. D.B. Robinson for his interest and guidance during this investigation.

Acknowledgement is made to F. Butz and his staff for their cooperation in building the equipment and to K. Balcombe for procuring the material necessary for its construction. The staff of the Computing Centre of the University of Alberta is thanked for their aid in the numerical calculations.

The author would like to give special thanks to R.A.S. Brown for his assistance in proof-reading the text and to typist Miss I. Tensfeldt. The financial assistance of the Pan American Petroleum Corporation through their graduate fellowship, and of the National Research Council is gratefully acknowledged.

TABLE OF CONTENTS

page

List of Tables i

List of Figures ii

INTRODUCTION 1

THEORY

- A Structure of Gas Hydrates 8
- B Statistical Theory of Gas Hydrates 17
  - (1) Partition Function 18
  - (2) Cell Partition 25
- C Phase Diagrams in Hydrate Systems 27
  - (1) Binary Systems 28
  - (2) Ternary Systems 30
  - (3) Hydrate Composition from Phase Diagrams 40
- D Prediction of Initial Hydrate Forming Conditions 46

EXPERIMENTAL

- A Experimental Equipment 49
  - (1) Equilibrium Cell 49

(2) Control and Measurement of Temperature 55

(3) Measurement of Pressure 57

(4) Equipment - General 58

(a) Valves and Tubing 58

(b) The Auxiliary Cell 59

(c) Mercury Cleaning 60

(d) Gas Purification 61

B Experimental Technique 63

(1) Charging the Equilibrium Cell 63

(2) Hydrate Formation 63

(a) The Binary System Sulfur Hexafluoride-Water Above 0°C 64

(b) The Binary System Sulfur Hexafluoride-Water Below 0°C 64

(c) The Ternary System Sulfur Hexafluoride-Methane-Water at -3°C 66

(3) Chromatographic Analysis 69

EXPERIMENTAL RESULTS

A The Binary System Sulfur Hexafluoride-Water 71

B The Ternary System Sulfur Hexafluoride-Methane-Water at -3°C 76

C Equilibrium Constants for Sulfur Hexafluoride and Methane at -3°C 79

D The Prediction of Initial Hydrate Forming Conditions 83

DISCUSSION 87

A The Ternary System Sulfur Hexafluoride-Methane-Water 87

B Relative Stability of Hydrate Structures 89

CONCLUSIONS 93

AREAS FOR FUTURE INVESTIGATION 95

NOMENCLATURE 96

BIBLIOGRAPHY 99

APPENDIX 102

A The Metastable Equilibrium of Hydrate-Gas-Ethylene Glycol Solution 103

B Tabulations 106

C Equipment Calibrations 115

LIST OF TABLES

page

I Experimental Pressure-Temperature Data for the System Sulfur Hexafluoride-Water 107

II Experimental Pressure-Composition Data for the System Sulfur Hexafluoride-Methane-Water at -3°C 108

III Data from the Theoretical Prediction of the Pressure-Composition Phase Diagram for the System Sulfur Hexafluoride-Methane-Water at -3°C 109

IV Equations from the Least Square Curve Fit of the Experimental Pressure-Temperature Data for the Sulfur Hexafluoride-Water System 110

V Equations for the Weighted Least Square Curve Fit of a Linear Curve 111

VI Calculation of the Heat of Formation of the Sulfur Hexafluoride Hydrate at 0°C 113

LIST OF FIGURES

page

I The Molecular Diameter of a Number of Compounds which Form Hydrates 6

II The Unit Cell of Structure I 9

III The Cavities in Structure I 11

IV A Model of the Unit Cell of Structure I 12

V The Large Cavity in Structure II 15

VI Pressure-Temperature Phase Diagram For a Typical Binary Hydrate System 29

VII Isothermal Cross-Section of the System $C_3H_8-H_2S-H_2O$ at -3°C 33

VIII Isothermal Cross-Section of the System $CH_4-C_3H_8-H_2O$ at -3°C 35

IX Pressure-Temperature Phase Diagram for a Typical Ternary Hydrate System 37

X Schematic Diagram of Equipment 50

XI The Assembled Equipment 51

XII The Equilibrium Cell 52

XIII The Agitation Mechanism 54

XIV Gas Purification Apparatus 62

XV Pressure-Temperature Phase Diagram for the System SF_6-H_2O 72

XVI Isothermal Cross-Section of the System SF_6-CH_4-H_2O at -3°C 77

XVII Equilibrium Constants for CH_4 at -3°C 81

XVIII Equilibrium Constants for SF_6 and C_3H_8 at -3°C 82

XIX Qualitative Effect of Ethylene Glycol on the Equilibrium HL_2G 104

XX Kromo-Tog Calibration for SF_6 116

XXI Kromo-Tog Calibration for CH_4 117

XXII Volumetric Calibration of the Equilibrium Cell 118

XXIII Volumetric Calibration of the Auxiliary Cell 119

XXIV Iron-Constantan Thermocouple Calibration 120

INTRODUCTION

In 1810, Sir Humphrey Davy formed a solid by cooling a saturated solution of chlorine in water to a temperature below nine degrees Centigrade. He called the solid a gas hydrate. Soon after, Faraday (6) used this solid to obtain liquid chlorine. He decomposed a quantity of chlorine hydrate contained in a sealed flask and chlorine was evolved until its partial pressure was greater than the vapor pressure of pure chlorine, thus causing a chlorine-rich liquid to appear. Further study of this and other gas hydrates was continued by Isambart (14), de Forcrand (7,8) and Villard (32). It was established that for a binary system the process

$$\text{water-rich liquid} + \text{gas} = \text{hydrate}$$

represented a univariant equilibrium. This means that at any given temperature where these three phases exist, the pressure of the system has a unique value. This can be confirmed by application of the phase rule which states that

$$f = c + 2 - p$$

where f is the number of degrees of freedom, p is the number of co-existing phases and c is the number of components present. It follows that, for any binary hydrate system, the number of degrees of freedom is one and the system is univariant along the three phase line where hydrate, water-rich liquid and vapor co-exist.

An accurate knowledge of the composition of gas hydrates was not obtainable for many years, largely because direct analysis led to ambiguous results due to decomposition of the hydrate and/or occlusion of mother liquor in the crystals. The failure of the molecules forming the hydrate to combine in the ratio of small integral numbers, as would be expected for normal chemical compounds, added to the controversy. The fact that 'non-integral ratios' were obtained experimentally was attributed to errors in analysis and it was not until Scheffer and Meyer (26) derived a method of indirect analysis that the 'non-integral ratios' were clearly verified for some cases. A detailed account of their analytical technique is given later.

The mechanism by which gas hydrates are formed became clear when von Stackelberg et al (28,29) succeeded in obtaining the X-ray diffraction patterns of a number of gas hydrates.

Claussen (2) assisted in determining structural arrays to fit these patterns. According to these authors, gas hydrates crystallize in either of two cubic systems referred to as Structure I and Structure II. In these structures the hydrated molecules are situated in cavities formed by a framework of water molecules which are linked by hydrogen bonds. The dimensions of the cavities differ for the two structures, but in both, the water molecules are tetrahedrally co-ordinated as in ordinary ice.

In general, the gas hydrate host lattice is thermodynamically unstable by itself and is stabilized by the solute molecule. The forces binding this component must be similar in nature to the intermolecular forces in liquids and van der Waals and Platteeuw (33) have concluded that the gas hydrates can be regarded as a solid solution of a second component in a metastable host lattice.

Palin and Powell (22,23), from their study of the curious "compounds" formed by hydroquinone with many gases and liquids, concluded that no chemical bonding occurred and that these types of substances were inclusion compounds. They called this type of compound a "clathrate" and defined it as a compound in which two (or more) components are associated not by ordinary

chemical union but through complete enclosure of the remaining components in a suitable structure formed from one component. They deduced that hydroquinone molecules, as a result of hydrogen bonding, formed two interpenetrating crystal structures which contained roughly spherical cavities in the ratio of one cavity for every three hydroquinone molecules. If the cavities are all vacant, then this crystal structure is called the metastable β modification of ordinary hydroquinone. The ordinary crystal lattice of hydroquinone is termed the α modification. When some of the cavities of the β crystal structure are occupied by suitable molecules, the structure becomes thermodynamically stable under certain conditions of temperature and pressure.

Before any structural information was available Nikitin (20) expressed the opinion that the binding mechanism of the gas hydrates was similar to that of the hydroquinone compounds. The X-ray analyses of gas hydrates by von Stackelberg and Muller (28,29) confirmed this opinion, thereby showing that gas hydrates are members of the family of clathrate compounds.

While it is difficult to predict accurately which molecules will form clathrate compounds, the principle is quite clear. Any molecule which can fit into the cavities will

stabilize the crystal lattice unless it shows specific chemical interaction with the host lattice. For instance, hydrogen chloride will not form a gas hydrate even though it has the correct size; instead, the compounds $HCl \cdot 2\ H_2O$, $HCl \cdot 3\ H_2O$ and $HCl \cdot 4\ H_2O$ are formed. However, HCl will readily form a hydroquinone clathrate. On the other hand, NH_3 does not form either a gas hydrate or a hydroquinone clathrate. Some of the molecular species which form hydrates together with their longest molecular dimension are shown in Figure I.

The peculiar behavior of forming a solid phase from either a liquid or solid host molecule and gaseous solute without chemical reaction has some beneficial advantages and applications. Recent research on the de-salination of sea water has shown that a method of producing salt-free water from the sea using gas hydrates is feasible. The technique involves the decomposition of hydrate originally formed from sea water. Another proposed application is the removal and storage of rare gas by-products from nuclear fission reactors. These uses have yet to be commercially exploited. The formation of hydrates by many of the components present in natural gases causes plugging of pipelines and equipment when favorable hydrate forming conditions are present. The prediction of

FIGURE I

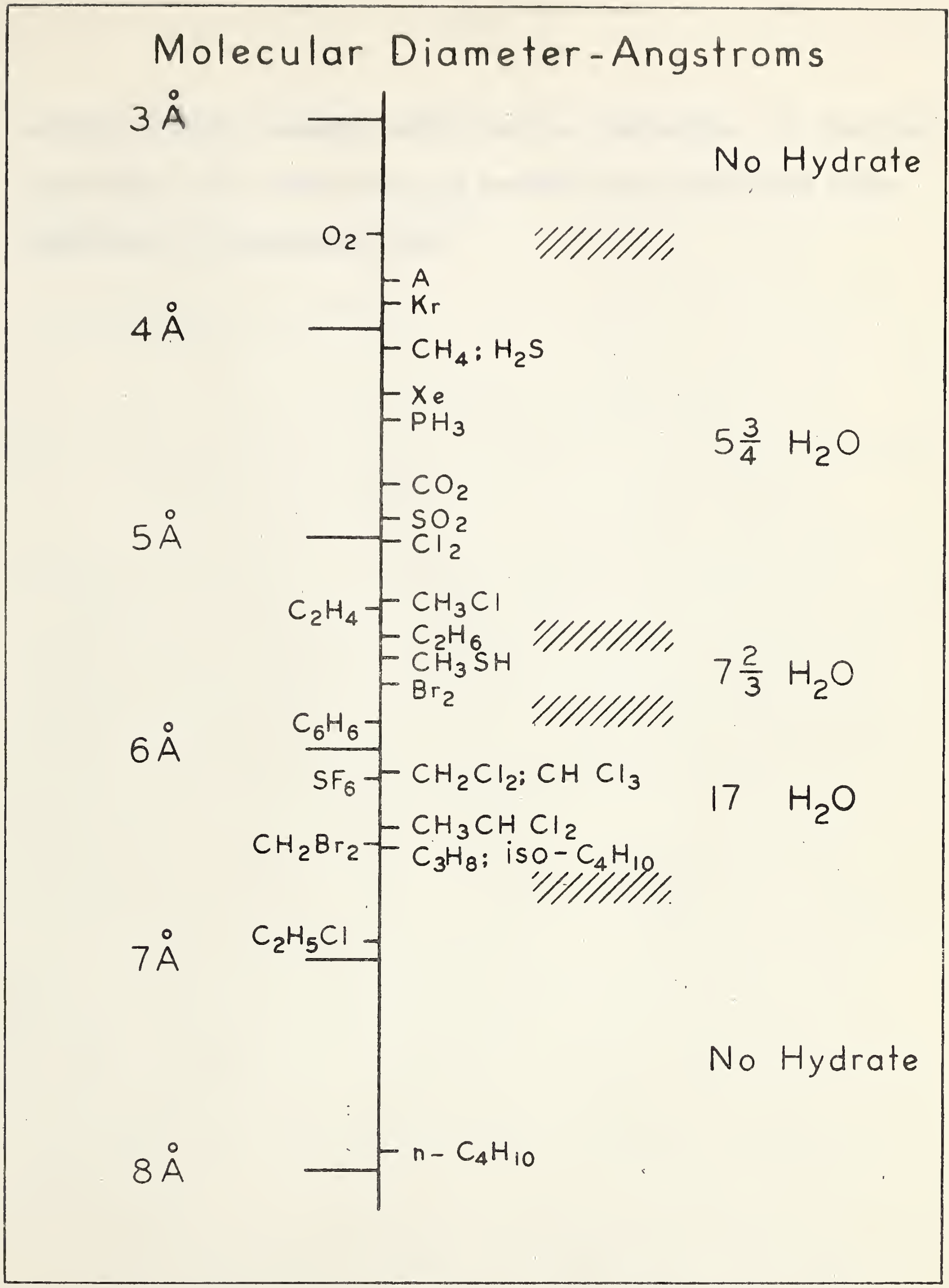

The Molecular Diameter of a Number of Compounds which form Hydrates

[illegible]

initial hydrate forming conditions is, therefore, of practical importance and a discussion of methods for predicting these conditions is presented later.

THEORY

A STRUCTURE OF GAS HYDRATES

As previously indicated, gas hydrates may form in either of two different crystal structures, I or II. Structure I has a unit cell containing 46 water molecules enclosing two types of cavities. The smaller cavities, situated at the vertices and the centre of the unit cell, are formed from 20 water molecules arranged in twelve pentagonal faces. The second cavity contains fourteen faces where two opposing hexagons are connected by twelve pentagonal arrays. The basic features of the unit cell of Structure I, according to von Stackelberg and Muller (29), are shown in Figure II. For the sake of clarity, only the elements lying in the nearer half are shown. The small dots represent the water molecules while the larger ones denote the centres of the two different types of cavities. The lines represent the hydrogen bonds of the lattice.

Figure III shows models of the two cavities which, when joined together, make up Structure I. The upper model

FIGURE II

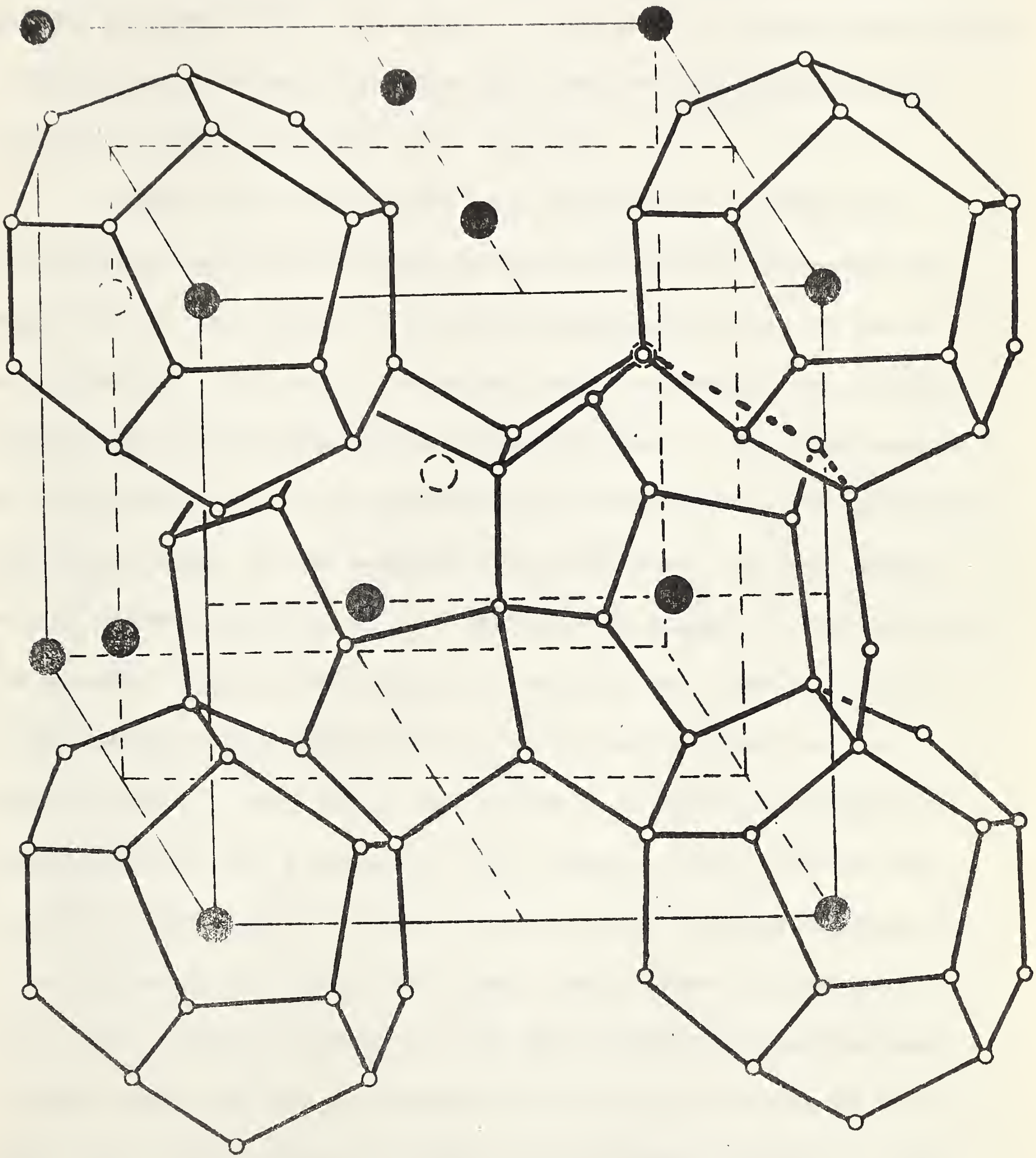

The Unit Cell of Structure I

represents the smaller cavity, a pentagonal dodecahedron formed from twelve identical pentagons. These cavities are almost perfectly spherical. The lower structure is a tetrakaidecahedron, in which, for better visualization, the two opposing hexagons are constructed from dark colored balls.

Figure IV shows a model of Structure I constructed from wooden balls and a combination of brass and polyethylene pegs fitted into holes drilled tetrahedrally into the surface of the balls. The balls represent water molecules (or oxygen atoms) and the pegs represent hydrogen bonds. The bond angles of Structure I are only approximately tetrahedral, the greatest deviation being in the hexagon structure with its bond angle of 120 degrees instead of the tetrahedral angle of 109½ degrees. For greater clarity only part of the unit cell was assembled; construction being restricted to the frontal plane and the central parts of the cell. Eight small cavities, pentagonal dodecahedrons, are situated at the corners, with a ninth one located at the centre. Three series of the tetrakaidecahedrons joined through the hexagonal faces, are present in the unit cell. The hexagonal faces of the three series are orthogonal to each other and are in planes parallel to the sides of the unit cell. The hexagonal faces of the larger cavities in the

FIGURE III

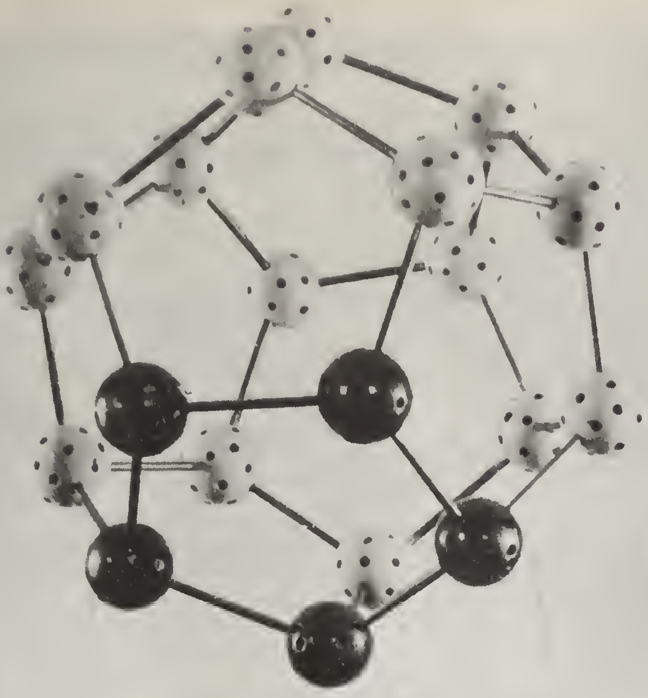

(a)

The Small Cavity in Structure I

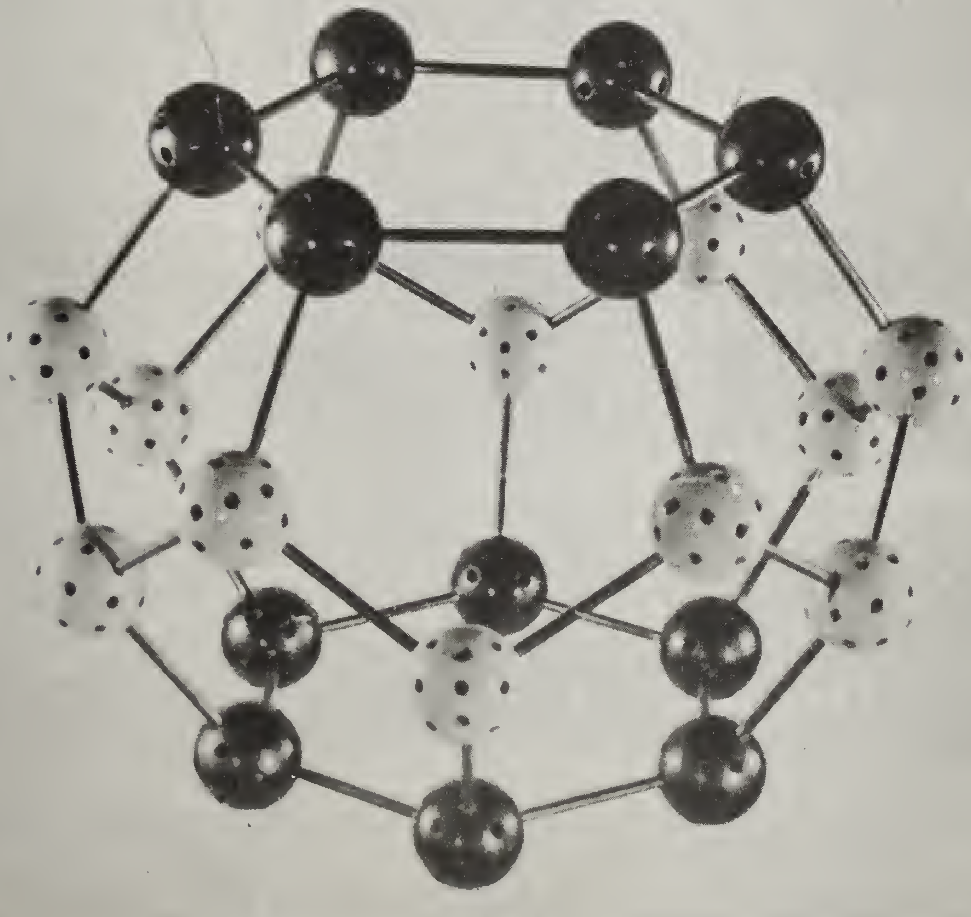

(b)

The Large Cavity in Structure I

FIGURE IV

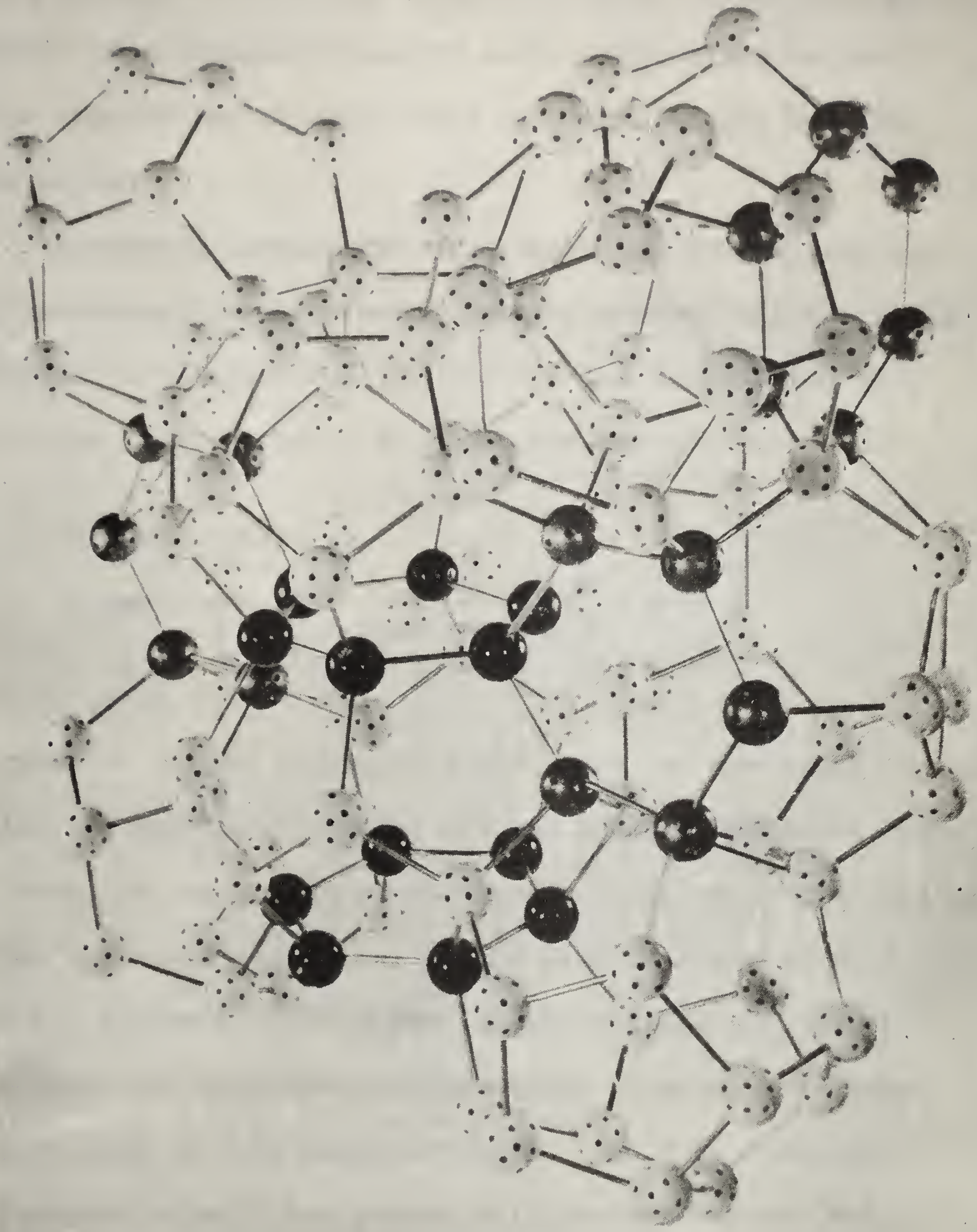

A Model of the Molecular Arrangement in a Unit Cell of Structure I

frontal plane are constructed of dark balls, outlining their position. One hexagonal face in each of the other series is also constructed of dark balls to emphasize the position of the series.

Agreement between the observed X-ray intensities and those calculated from the model are not perfect but the latter is thought to be essentially correct. The composition of a gas hydrate of Structure I is then characterized by:

46 water molecules
2 small cavities $z_1 = 20$ $r_1 = 3.95$ Å
6 larger cavities $z_2 = 24$ $r_2 = 4.30$ Å

The number of oxygen molecules surrounding the two types of cavities are denoted by z_1, z_2 and the average distances from these atoms to the centre of the cavity by r_1, r_2. The smaller cavities are nearly spherical with a free diameter of approximately 5.1 Angstrom units. The larger cavities are somewhat oblate since the distances of the oxygen atoms to the centre vary from 4.04 to 4.65 Angstrom units. The free diameters were computed using 1.4 Angstrom units as the van der Waals radius for oxygen.

The unit cell for Structure II consists of 136 water molecules and is more complicated. The smaller cavities are distorted pentagonal dodecahedra with the distance from the oxygen atoms to the centre ranging from 3.77 to 3.95 Angstroms. The free diameter of this cavity is only 5.0 Angstrom units. The larger cavity is almost a perfect sphere with the oxygen atoms occupying the vertices of a hexakaidecahedron which has a free diameter of 6.7 Angstrom units. Figure V shows a model of this cavity which consists of four hexagonal faces connected by twelve pentagons. Two of the hexagonal faces have been constructed from dark balls for emphasis. The unit cell is characterized by:

136 water molecules
16 smaller cavities $z_1 = 20$ $r_1 = 3.91$ Å
8 large cavities $z_2 = 28$ $r_2 = 4.73$ Å

Hydrates of Structure II are formed only by those molecules which are too large to enter the Structure I lattice. This implies that they occupy only the larger cavities. In ternary systems consisting of two gaseous species and water, the terms "double" and "mixed" hydrates were proposed by von Stackelberg to describe the hydrates formed. "Mixed" hydrates referred

FIGURE V

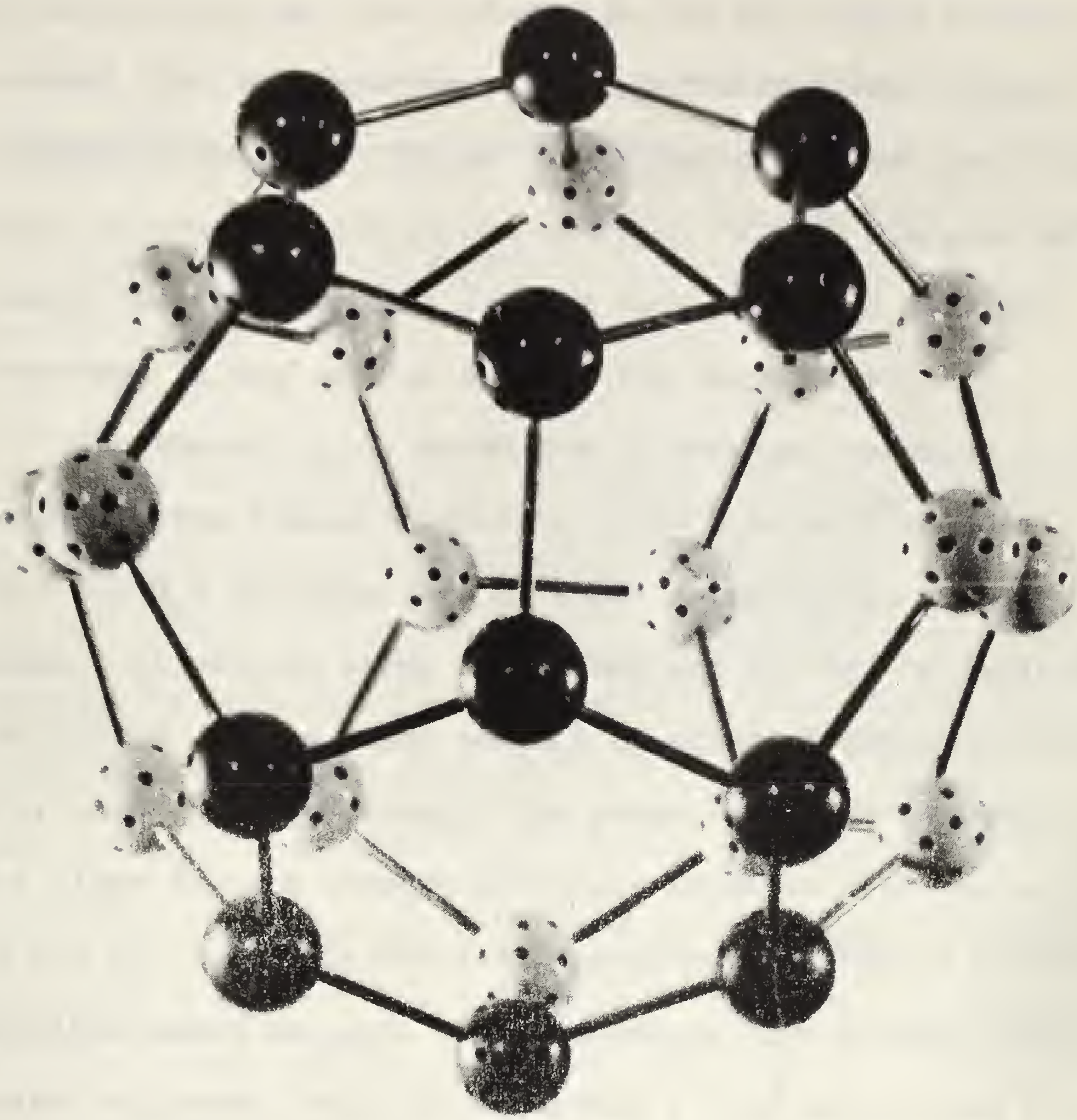

The Large Cavity of Structure II

to those ternary systems in which the binary systems crystallize in the same structure and "double" hydrates referred to systems where both structures were present in the two binary systems. He assumed that two separate crystal structures were present in a "double" hydrate. Van der Waals has shown that the "double" hydrates of von Stackelberg are actually "mixed" hydrates with the small molecular species fitting into the small cavities of Structure II was well as some of the larger cavities.

The theoretical composition of hydrates assuming that all cavities are filled would be $A \cdot 5\ 3/4\ H_2O$ for Structure I and $A \cdot 5\ 2/3\ H_2O$ for Structure II where A represents a gas molecule. It will be shown later that not all of the cavities can be filled and the water content of actual hydrates must be greater than the theoretical. The presence of two different cavity sizes in each crystal structure requires that the molecules which can fit into only the large cavities must have a greater theoretical water content. For a molecule like bromine which occupies the large cavity of Structure I, the theoretical water content is 7 3/4 while for Structure II, the limit is 17. Sulfur hexafluoride with its molecular diameter of 6.17 Angstrom units is too large by 0.4 Angstroms to enter the Structure I lattice and must necessarily form in Structure II where the

large cavities can accommodate it. The hydrate crystal must therefore contain more than 17 water molecules per molecule of sulfur hexafluoride.

B THE STATISTICAL THEORY OF GAS HYDRATES

Van der Waals and Platteeuw have constructed a model for clathrates on the basis of statistical mechanics. Only the final results and their direct application to the gas hydrates will be presented. For a detailed account, the reader is referred to the original publications (33,34).

The thermodynamic properties of clathrates were derived from a simple model which corresponds to the three dimensional generalization of ideal localized adsorption. A clathrate crystal of cage-forming substance Q and a number of encaged compounds ("solutes") A, B, ... M were considered. The substance Q has two forms: a stable modification (α) which under given conditions may be either crystalline or liquid and a metastable modification (β) enclosing cavities of different types 1, 2, ... n which acts as a host lattice in the clathrate. The number of cavities of type "i" per molecule of Q is denoted by "v". For gas hydrates of Structure I I $v_1 = 2/17$ and $v_2 = 1/17$.

The model is restricted by the following assumptions:

(1) The encaged molecules do not seriously distort the host lattice.

(2) The encaged molecules are localized in the cavities and each cavity is assumed to hold not more than one molecule.

(3) The mutual interaction of the enclosed molecules can be neglected.

(4) The principles of classical mechanics apply.

The restriction of assumption (1) is not severe since the host lattice is rigidly held by hydrogen bonds and the weak bonds of the included molecules will distort the crystal very little. Assumption (2) is valid as far as is known although a clathrate with multiple occupancy may form if the crystal structure has large cavities and the solute is small. However, no hydrates of the small molecules, neon, hydrogen and helium have yet been reported. The third assumption is not strictly correct but the solute molecules are separated by a Q molecule and it has been shown (5) that the solute interaction is quite small.

1 The Partition Function

A partition function was constructed to characterize the general clathrate system. For the gas phase both energy and particles were allowed to flow to and from the ensemble

making the function a grand partition function with respect to the gas phase. Since only energy flows across the ensemble boundaries of the Q crystal, the partition function is an ordinary one for the host lattice. Considering a system consisting of a clathrate crystal with more than one type of cavity containing several different molecular types, van der Waals and Platteeuw have obtained the following grand partition function, P.F.

$$\text{P.F.} = \exp\left(-\frac{F^{\beta}}{k\ T}\right) \prod_{i} \left(1 + \sum_{J} h_{Ji}\ L_J\right)^{v_i\ N_Q} \tag{1}$$

where F^{β} is the free energy of the "empty" β lattice for the given values of temperature T, volume V and number N_Q of molecules of Q; k is the Boltzmann constant; L_J is the absolute activity of the Jth solute molecule and h_{Ji} is the partition function of the Jth molecule when occupying a type "i" cavity.

From the grand partition function, two equations relating the clathrate composition, the partial pressure of each hydrate former, and μ, the chemical potential of the solvent may be derived:

$$y_{Ki} = C_{Ki}\ p_K \ /\ \left(1 + \sum_{J} C_{Ji}\ p_J\right) \tag{2}$$

$$\mu_Q = \mu_Q^{\beta} + kT \sum_i v_i \ln (1 - \sum_K y_{Ki}) \qquad (3)$$

In equation (2), y_{Ki} is the fraction of "i" cavities which are occupied by type K molecules; p_K is the partial pressure of K in the vapor phase assuming ideal gas behavior (for non-ideality, the partial pressure must be replaced by the fugacity); and C_{Ki} is defined by the following equation:

$$C_{Ki} = h_{Ki} L_K/p_K \qquad (4)$$

According to van der Waals and Platteeuw, L_K is a function of p_K, T and the molecular partition function, Θ_K, of gaseous K with the volume factor removed. Since the activity of K is not a function of volume, the removal of the volume term from Θ will make the activity a function only of temperature. The molecular partition function has been determined by many authors for various gaseous systems and Dale (4) has an extensive compilation. Van der Waals and Platteeuw's equation for the activity is:

$$L_K = p_K/kT\Theta_K \qquad (5)$$

By combining equations (4) and (5) the final form of C_{Ki} is

derived:

$$C_{Ki} = h_{Ki}/kT\Theta_K \tag{6}$$

In this expression h_{Ki} is a function of T and V and Θ is a function of T alone making C_{Ki} dependent upon T and V.

In equation (3) μ_Q is the chemical potential of the clathrate and μ_Q^β is the chemical potential of the "empty" β lattice of the host molecules. For stability of the clathrate with respect to Q^α, the normal state of the host molecules, the relation

$$\mu_Q \leqslant \mu_Q^\alpha \tag{7}$$

must be satisfied. At equilibrium

$$-\Delta\mu/kT = \sum_i v_i \ln(1 - \sum_K y_{Ki}) \tag{8}$$

where

$$\Delta\mu = \mu_Q^\beta - \mu_Q^\alpha \tag{9}$$

Equations (2) and (3) give an adequate description of the thermodynamic behavior of clathrate compounds and their application to gas hydrates follows directly. As an example,

let us consider a hydrate of Structure II in which two molecular species, A and B, occupy the cavities. Species A can occupy both cavities but B can only enter the larger one. Applying equation (2) to this situation results in the following set of equations which determine the fraction of each type of cavity that will be occupied by each species:

$$y_{A1} = \frac{C_{A1}\, p_A}{1 + C_{A1}\, p_A} \tag{2a}$$

$$y_{B1} = 0 \tag{2b}$$

$$y_{A2} = \frac{C_{A2}\, p_A}{1 + C_{A2}\, p_A + C_{B2}\, p_B} \tag{2c}$$

$$y_{B2} = \frac{C_{B2}\, p_B}{1 + C_{A2}\, p_A + C_{B2}\, p_B} \tag{2d}$$

The coefficient C_{B1} is zero since the large molecule B cannot fit into the small cavity.

The composition of the hydrate, Y moles of gas per mole of water, can be expressed as a function of the fraction of cavities which are occupied and the number of cavities per host molecule, i.e. the y_{Ki} and the v_i values.

$$Y_A = v_1\, y_{A1} + v_2\, y_{A2} \tag{10a}$$

$$Y_B = v_2\, y_{B2} \tag{10b}$$

Applying equation (3) completes the description as follows:

$$-\frac{\Delta\mu^{II}}{k\ T} = v_1 \ln (1 - y_{A1}) + v_2 \ln (1 - y_{A2} - y_{B2}) \tag{3a}$$

If the values of C_{Ki} and $\Delta\mu^{II}$ are known, the above equations can be used to determine hydrate composition. The calculation of C_{Ki} is possible if an adequate potential model describing a solute molecule in a cavity can be formulated. The theoretical calculation of $\Delta\mu$ is quite difficult and no literature on the subject has been published.

Two methods for determining $\Delta\mu$ are available: one semi-theoretical and the other experimental. Consider a molecule which will fit into the large cavity only. For one species of hydrating molecule B, the equations (2) and (3) reduce to:

$$y_{B2} = \frac{C_{B2}p_B}{1 + C_{B2}p_B} \tag{2e}$$

$$-\frac{\Delta\mu}{k\ T} = v_2 \ln (1 - y_{B2}) \tag{3b}$$

From equation (3b) it follows that $\Delta\mu$ is completely determined by the value of y_{B2} at any temperature. The experimental approach

is to determine the hydrate composition using the technique of Scheffer and Meyer (26) which is discussed in detail later and to calculate $\Delta\mu$ directly from equations (3b) and (10b). However, the method that Scheffer and Meyer developed is applicable only at zero degrees Centigrade where hydrate, aqueous liquid, ice and vapor are in equilibrium. The calculation of $\Delta\mu$ at slightly lower temperatures is quite easy because the solubility of gas in ice is essentially zero and therefore no solubility correction is required. More complex corrections must be made above zero degrees Centigrade because the potential of the liquid water phase will be influenced by the solubility of the hydrating molecules in it.

The semi-theoretical approach requires the calculation of C_{B2} from theoretical considerations and the experimental determination of the equilibrium pressure of the hydrate at the temperature of interest. Using these values and equations (2e) and (3b), y_{B2} and $\Delta\mu$ may be determined. The calculation of C_{B2} will be discussed in some detail later.

Miss Mulders (19) has determined the composition of the bromine hydrate to be 8.47 plus or minus 0.05 molecules of water per molecule of bromine at zero degrees Centigrade. She employed the technique of Scheffer and Meyer to obtain this

result. Since bromine crystallizes only in the large cavities of Structure I, the values of $\Delta\mu^{I}$ and C_{B2} follow directly from equations (2e), (3b) and (10b). As previously mentioned, the molecular dimensions of sulfur hexafluoride restrict it to the larger cavities of Structure II only and one of the objectives of this work was to obtain $\Delta\mu^{II}$ from a determination of the composition of the sulfur hexafluoride hydrate at zero degrees Centigrade by the method of Scheffer and Meyer.

2 The Cell Partition Function

The grand partition function and the resulting equations contain the cell partition function h_{Ji}. From X-ray analysis it appears that the cavities are nearly spherical with walls containing large numbers of molecules. Therefore it seems reasonable to suppose that the solute molecules are surrounded by a force field having spherical symmetry. Based on Assumptions (1) - (4) and on the following assumptions, Lennard-Jones and Devonshire (16) have developed a method of evaluating the partition function of a molecule in a spherical cavity from a mathematical representation of the resultant potential energy field within the cavity.

(5) The solute molecules rotate freely in the cavities i.e. the rotational partition function is the same as that in the perfect gas.

(6) The potential energy of a solute molecule may be represented by the spherically symmetrical energy potential proposed by Lennard-Jones and Devonshire.

With the imposition of the last two restrictions, the applicability of the theory becomes limited, although it must be emphasized that the equations derived using Assumptions (1) to (4) are quite general in scope. Strictly speaking, with the additional restrictions the theory is applicable only to the monatomic gases and to a lesser extent, to the almost spherical molecules CH_4, CF_4 and SF_6.

The Lennard-Jones and Devonshire potentials have the form

$$X(R) = 4\,\varepsilon\left((\sigma/R)^{12} - (\sigma/R)^{6} \right) \qquad (11)$$

where X is the potential energy between the solute molecule and one of the surrounding molecules. It is a function only of R, the distance between the solute and the particular wall element. The energy and distance parameters ε and σ refer to the specific species involved; σ being the distance for which attraction and repulsion are equal, i.e. $X(\sigma) = 0$, and ε is the value of $-X(R)$ corresponding to the strongest attraction which occurs at $R = 2^{1/6}\,\sigma$.

Lennard-Jones and Devonshire summed the interaction over z molecules distributed over the surface of a sphere and obtained a function describing the resultant field within the sphere averaged over all orientations. The precise form of this function and its relation to h_{Ki} is given by Lennard-Jones and Devonshire (16), Fowler and Guggenhiem (9) and van der Waals and Platteeuw (33). From the h_{Ki} , values of C_{Ki} can be determined using equations (5) and (6). Van der Waals and Platteeuw have calculated these constants for a number of solute molecules enclosed in a water crystal structure. Their results for sulfur hexfluoride and methane are used in this work.

C PHASE DIAGRAMS IN HYDRATE SYSTEMS

The conventional method of presenting phase equilibria in gas hydrate systems is in the form of phase diagrams with pressure or the logarithm of pressure as the ordinate and temperature as the abscissa. With five or six phases appearing on the phase diagram, a wide variety of equilibria are possible. In binary systems the univariant lines represent three phase equilibria and separate the diagram into regions where two phases co-exist. The intersection of these lines will form non-variant points where four phases are in equilibrium. When

the number of components is increased to three, the diagram becomes more complex with the univariant lines representing four phase equilibria and the non-variant points representing five phases in equilibrium. The different phase diagrams are discussed in detail below using the following nomenclature:

H_I - hydrate of Structure I
H_{II} - hydrate of Structure II
L_1 - non-aqueous liquid
L_2 - aqueous liquid
I - ice
G - gas

1 Binary Systems

Figure VI depicts a typical phase diagram for a two component system in which the critical point of the solute is above the hydrate forming conditions. Two quadruple points are present denoting the solid-liquid phase change for water at A and the gas-liquid phase change for the hydrate former at B. The equilibrium HGL_2 is terminated at B where H, L_1 , L_2 and G are in equilibrium. The temperature of the liquid-solid equilibrium, L_1 L_2 H which originates at B, is almost unaffected by pressure and hydrate will not form at temperatures much above this quadruple point temperature. Examples of this

FIGURE VI

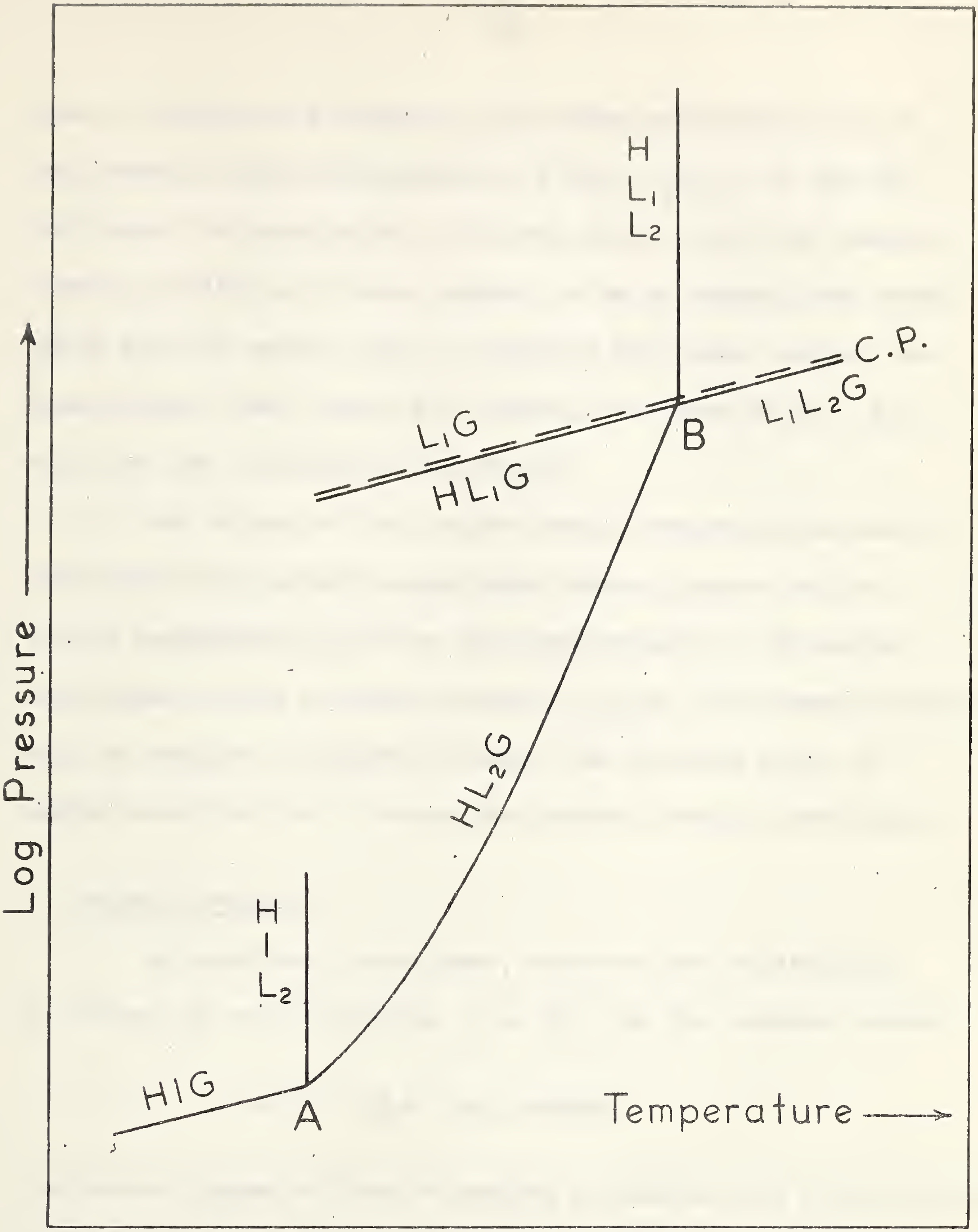

Pressure - Temperature Phase Diagram for Typical Binary System where the Critical Point is Above the Hydrate Forming Conditions

type of diagram are numerous, including practically all of the hydrates with the exception of CH_4, C_2H_4,A, Kr and Xe. For these few gases with a critical point below the hydrate forming conditions, there appears to be no temperature above which hydrate cannot exist. Diagrams for these species are much simpler than Figure VI, lacking the lines HL_1G, L_1L_2G, HL_2G and the quadruple point HL_1L_2G.

One object of this experimental investigation was to determine the pressure-temperature phase diagram for the sulfur hexafluoride hydrate from approximately -10 degrees Centigrade to the quadruple point $H_{II}L_1L_2G$. The phase diagram will be similar to Figure VI since the critical point of sulfur hexafluoride is above the hydrate forming conditions.

2 Ternary Systems

As previously mentioned, hydrates can crystallize in either of two structures, I or II. For the ternary system

$$A + B + H_2O \rightleftharpoons \text{Hydrate}$$

the phase diagram differs depending on whether the binary systems A + H_2O and B + H_2O crystallize in the same type of structure or not.

Systems crystallizing in one type of structure are characterized by complete miscibility of the solid solutions with compositions ranging continuously from pure A hydrate to pure B hydrate. Von Stackelberg and Meinhold (30) found complete miscibility for the systems C_2H_5Cl-$C_2H_4Cl_2$-H_2O and C_2H_5Cl - $CHCl_3$-H_2O when they determined the composition of L_1 (on a water free basis) as a function of temperature at atmospheric pressure in the three phase region $L_1L_2H_{II}$. Reamer, Selleck and Sage (25) found similar behavior from their studies on the propane-propylene-water system. They were able to construct a temperature-composition phase diagram at 400 psi which clearly demonstrated that complete mixing occurred in the $L_1L_2H_{II}$ region.

A pressure-temperature phase diagram for ternary systems may be constructed by joining the corresponding quadruple points of the binary systems by the four phase lines HIL_2G and HL_1L_2G.

Where the binary systems crystallize in different structures, partial miscibility will occur in the solid phase of the ternary system. This is clearly demonstrated by the H_2S-C_3H_8 hydrate studied by Platteeuw and van der Waals (24). A reproduction of their experimental pressure-composition diagram at -3 degrees Centigrade, with composition on a water-free

basis, is presented in Figure VII. The regions of complete miscibility in Structure II and in Structure I, and partial miscibility, denoted by the presence of the two hydrate structures together, is clearly shown. The diagram exhibits a minimum pressure where the gas and hydrate equilibrium lines have a common tangent analogous to azeotropy in vapor-liquid equilibria. This behavior was predicted by Platteeuw and van der Waals from the statistical mechanical model for gas hydrates and, although the predicted diagram did not coincide exactly with experiment, the essential features were present. That considerable deviation occurred is not surprising since H_2S is a polar molecule and neither the H_2S nor the C_3H_8 molecules are spherical. Therefore, the restrictions inherent in the Lennard-Jones and Devonshire potential theory were not obeyed and the calculated cell partition functions must necessarily be in error. However, the prediction of the "azeotrope" demonstrates the validity of the theory which has been proposed for gas hydrates.

A further example where the assumptions of the Lennard-Jones and Devonshire theory were obeyed to a greater extent is in the methane-propane hydrate studied by van der Waals and Platteeuw (33) at -3 degrees Centigrade. Figure VIII is

FIGURE VII

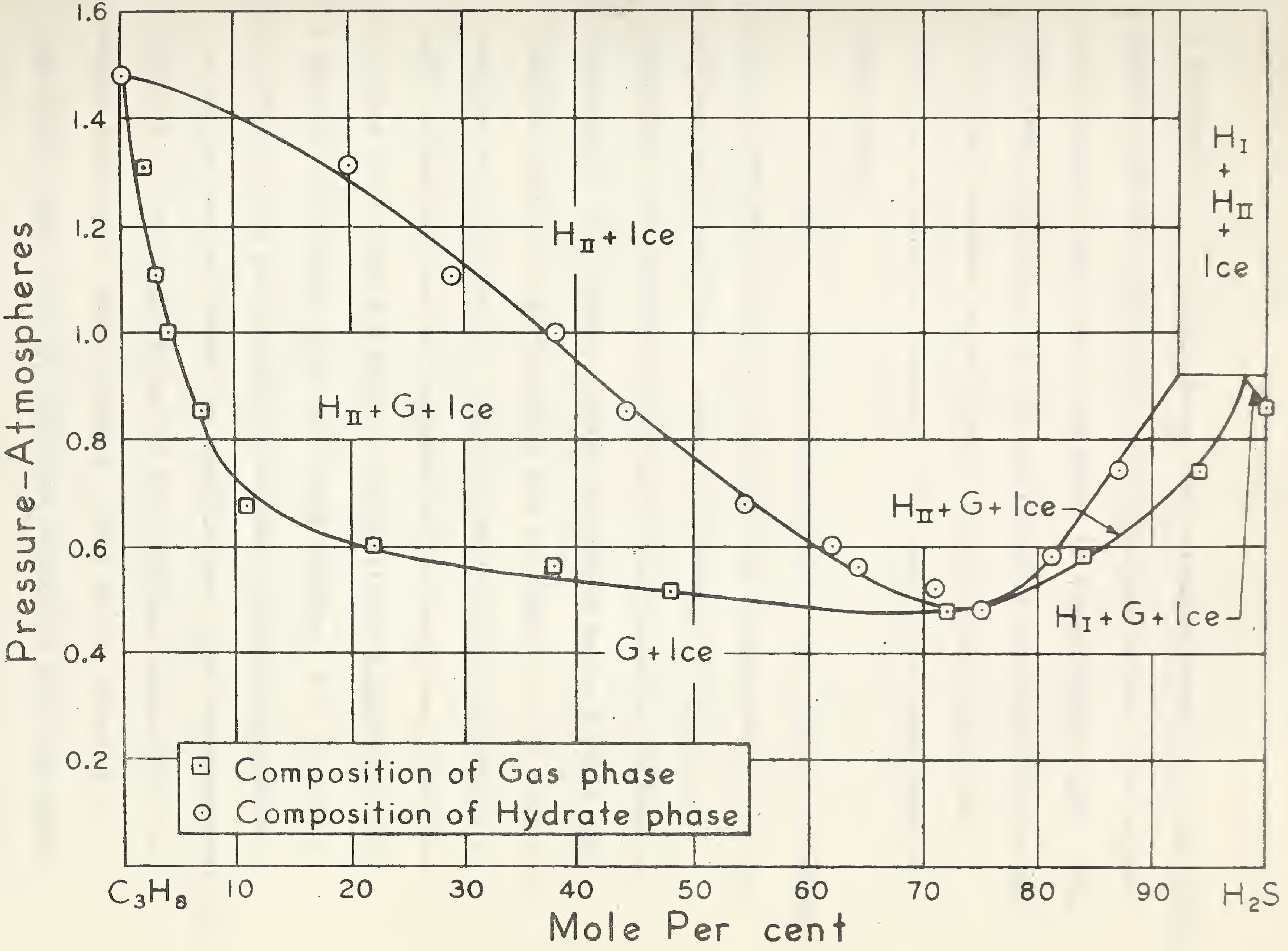

Isothermal cross-section of the system $C_3H_8-H_2S-H_2O$ on a water-free basis at -3°C.

a reproduction of their data, the points representing experimental results and the solid lines the predicted curves. The agreement between theory and experiment is surprisingly close. The very large difference in the equilibrium pressures between the two binary systems significantly reduced the region where Structure I alone is present. The inset is an expansion of this region.

In both of the previous examples, the region of complete miscibility in Structure II hydrate was terminated by the appearance of a new phase, namely a hydrate of Structure I. Apparently the preferred structural configuration is that of Structure I, the second crystal structure being formed only when the stabilizing molecules are too large to fit into the cavities of Structure I. In a ternary system containing a small molecular species together with a large one, Structure II alone will form for hydrate compositions beginning with a hydrate containing only the large species, i.e. a binary system. As the percentage of the small species increases, a point is reached where the equilibrium $H_{II}IG$ becomes metastable relative to the equilibrium of both hydrate phases with ice. Beyond this point both H_I and H_{II} will exist, forming a three phase region $H_IH_{II}I$, which is separated from the three

FIGURE VIII

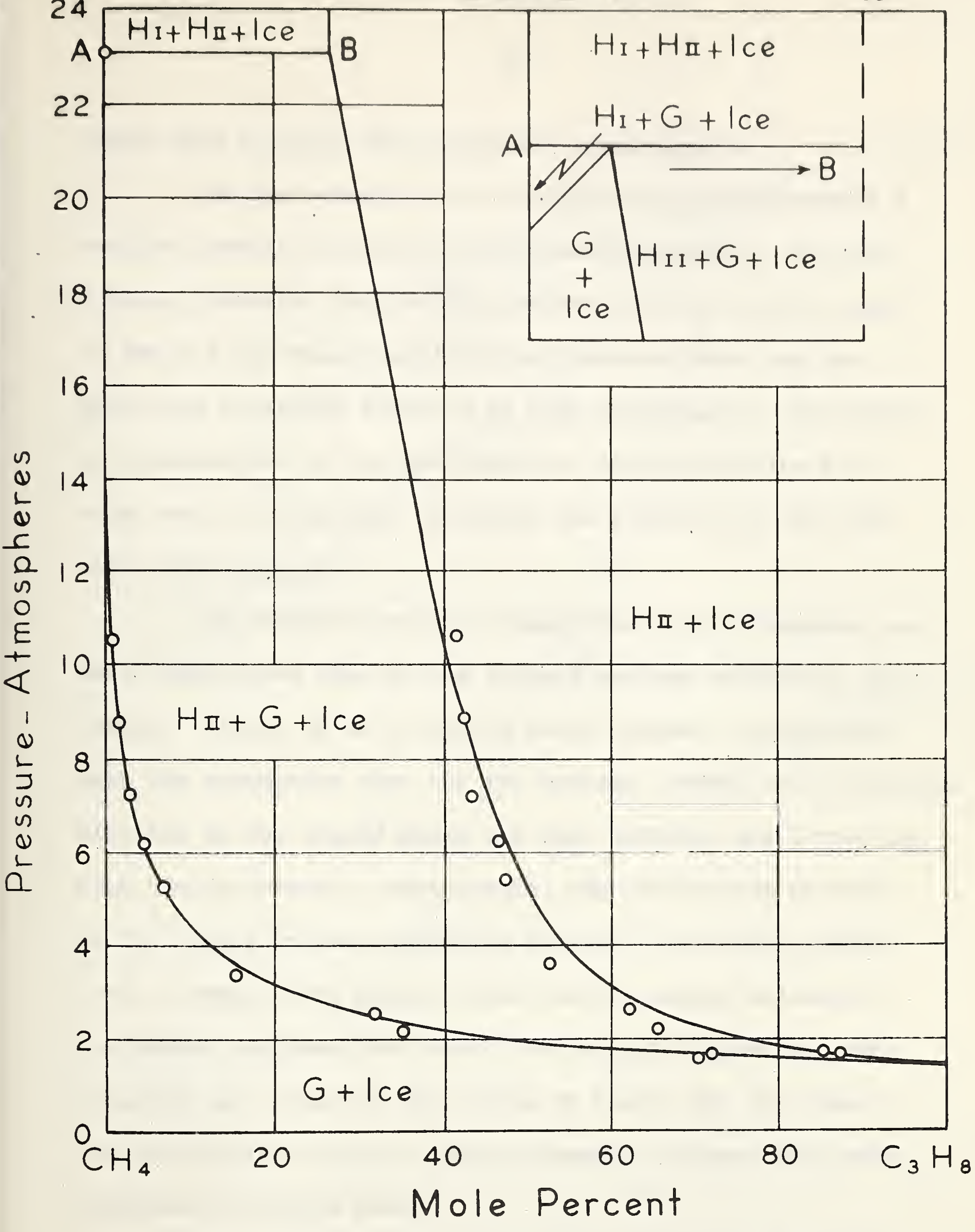

Isothermal Cross-Section of System $CH_4-C_3H_8-H_2O$ on a Water-Free Basis at -3 °C

phase area $H_{II}GI$ by the four phase line $H_IH_{II}IG$.

The gas branch of the equilibrium H_IIG represents a constant partial pressure of the smaller species. In the H_2S-C_3H_8 hydrate, the partial pressure of H_2S must be equal to the H_2S-H_2O binary equilibrium pressure which van der Waals and Platteeuw found to be 0.86 atmospheres. The point of intersection of the gas branch of the equilibrium H_IIG with that of $H_{II}IG$ will determine the position of the four phase line $H_IH_{II}IG$.

The complete pressure-temperature phase diagrams are more complicated than in the ternary systems previously discussed. Figure IX is a typical phase diagram, constructed with the assumption that the two hydrate formers are completely miscible in the liquid phase and that hydrates are formed in both binary systems. Furthermore, the equilibrium pressure of the binary system containing the small molecular species A was assumed to be greater than for the larger molecule B. The binary diagrams from which the ternary diagram was constructed, are drawn in thin lines on Figure IX; the vapor-liquid equilibria of the single-component systems have been indicated by dotted lines.

The ternary diagram was constructed from the binary

FIGURE IX

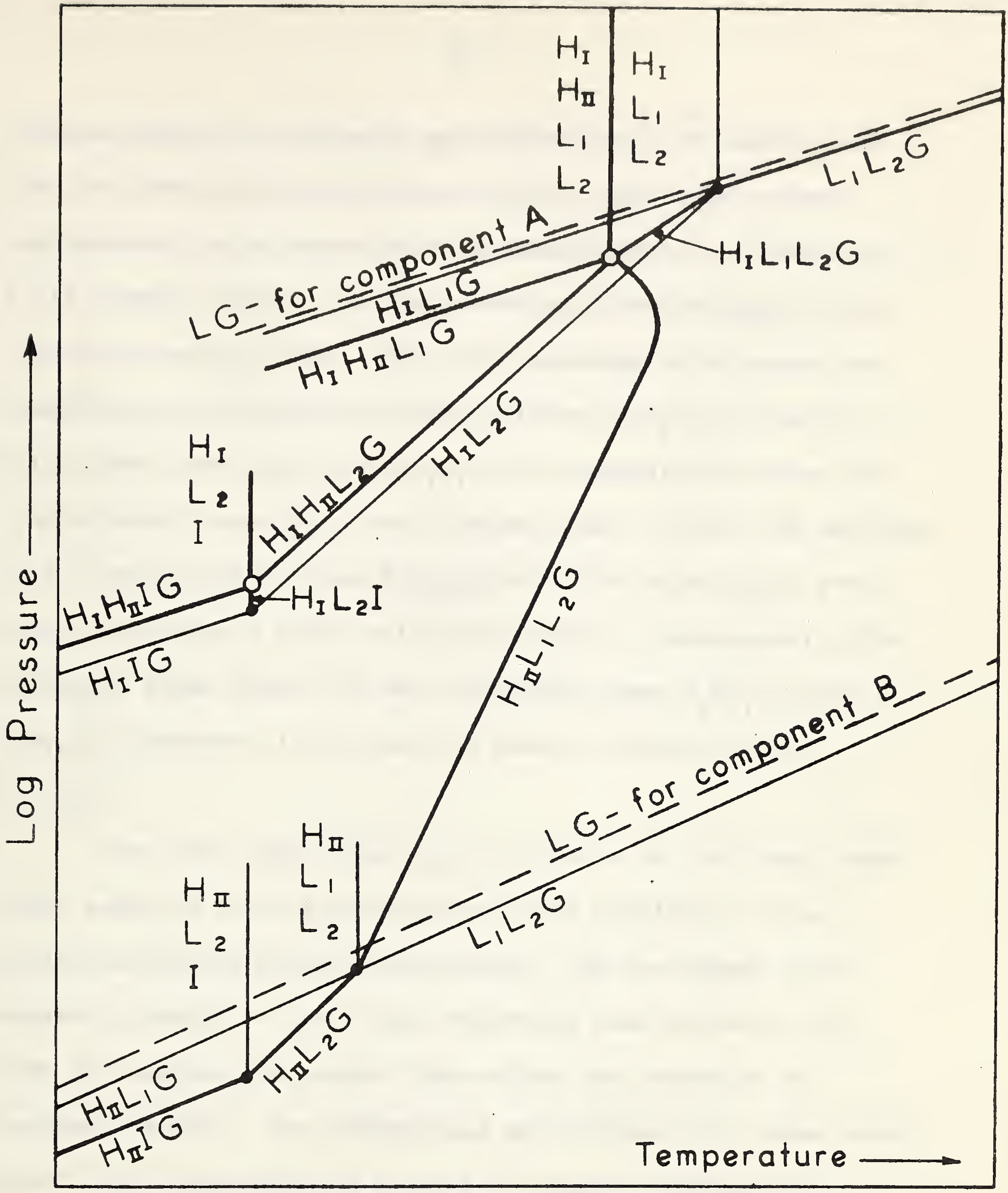

Pressure-Temperature Phase Diagram for a Typical Ternary System, A-B-H_2O, in which Hydrates of Different Structures are Formed in the Binary Systems A-H_2O and B-H_2O

diagrams using the following considerations. On addition of B to the three phase equilibrium $H_{I}IG$ in the A-H_2O system, the pressure is increased until a mixed hydrate of Structure II is formed. Hence, the four phase equilibrium $H_{I}H_{II}IG$ must lie above the $H_{I}IG$ line. The same reasoning holds above the freezing point of water for the position of $H_{I}H_{II}L_2G$ versus $H_{I}L_2G$. The lines $H_{I}L_1G$ and $H_{II}L_1G$ will probably lie below the liquid-vapor lines for A and B respectively. After the addition of B, the four phase line $H_{I}H_{II}L_1G$ will lie below $H_{I}L_1G$ since water and B have a lower volatility than A. Consequently, the quintuple point where the two four-phase lines $H_{I}H_{II}L_1G$ and $H_{I}H_{II}L_2G$ intersect lies below the binary quadruple point $H_{I}L_1L_2G$.

The four phase line $H_{II}L_1L_2G$ begins at the binary quadruple point of the B-H_2O system and must terminate at the quintuple point previously mentioned. The four phase line appears to bulge to the right indicating that hydrates will form at temperatures higher than either the quintuple or quadruple points. Von Stackelberg and Fruhbuss (31) have determined this temperature to be near 33 degrees Centigrade for the system CCl_4-H_2S-H_2O, approximately 7 degrees above the estimated quintuple point temperature.

Agreement between the theory proposed for gas hydrates and experiment has been demonstrated by van der Waals and Platteeuw through their experimental determination and theoretical prediction of the pressure-temperature phase diagrams on a water-free basis for the ternary hydrate systems previously mentioned. The agreement between the experimental and predicted diagrams indicates that the theory is essentially correct.

Van der Waals and Platteeuw studied ternary systems in which one of the hydrate formers could fit only into the larger cavities of the particular hydrate structure considered. Equations (2a,b,c,d) and (3a) are applicable to these systems. Assuming that

$$p_A = x\ P \qquad (12)$$

where x is the mole fraction of A in the gas phase and P is the total pressure, then equation (3a) may be written in the following form.

$$\exp\ (17\Delta\mu^{II}/RT) = (1 + C_{A1}xP)^2\ (1 + C_{A2}xP + C_{B2}(1 - x)P) \qquad (13)$$

If the $\Delta\mu^{II}$ and C values are known at the temperature of interest, then equation (13) becomes a function of P and x and the pressure-composition diagram may be constructed using

equations (2a,b,c,d) and (13).

A comparison of the experimental and predicted pressure-composition phase diagrams for sulfur hexafluoride-methane hydrate at -3 degrees Centigrade was one objective of this investigation. The system is similar to the propane-methane hydrate studied by van der Waals and Platteeuw and a similar type of diagram should result.

3 Hydrate Composition From Phase Diagrams

Scheffer and Meyer (26) have developed an indirect thermodynamic method for determining the composition of gas hydrates at zero degrees Centigrade. In essence the product of the molal heat of fusion of water and the number of moles of water associated with one mole of gas is equal to the difference between the heat of formation of the hydrate from ice and from water at zero degrees Centigrade. The heats of formation are determined from the Clapeyron equation.

The Clapeyron equation is applicable to any univariant equilibrium and may be summarized in the following form:

$$\frac{dP}{dT} = \frac{\Delta h}{T\Delta V} \qquad (19)$$

P = pressure

T = absolute temperature

ΔV = change in volume of the system accompanying the phase change

Δh = change in enthalpy that the system undergoes during the phase change

The numerical value of the enthalpy change during formation or decompostion is the same but of opposite sign. For the sake of simplicity, the case of decomposition is considered.

For a hydrate system

$$\Delta V = V_G + V_{L_2} - V_H \tag{15}$$

where V_G and V_{L_2} refer to the volumes of the gas and liquid water or ice that result from hydrate decomposition and V_H is the volume of hydrate. V_H and V_{L_2} are approximately equal and, since V_G is very much larger than either, the error introduced by replacing ΔV with V_G is negligible.

Corrections to the value of Δh from the Clapeyron equation must be made to account for the solubility of hydrate former in water and the evaporation of sufficient water to saturate the gas volume produced by the decomposition.

The phase change along the equilibrium HL_2G in Figure VI may be simplified into three separate steps:

(1) decomposition of hydrate into pure gaseous hydrate former A and pure liquid water;

(2) evaporation of sufficient water to saturate the vapour phase and

(3) the saturation of water with A.

These steps in equation form are:

$$A \cdot nH_2O \rightleftharpoons A(G) + n\ H_2O(L) \qquad - \triangle h_{decomposition} \qquad (16)$$

$$r\ H_2O(L) \rightleftharpoons r\ H_2O(G) \qquad - \triangle h_{evaporation} \qquad (17)$$

$$s\ A(G) + (n - r)\ H_2O \rightleftharpoons \text{solution} \qquad - \triangle h_{solution} \qquad (18)$$

In this terminology, $A \cdot nH_2O$ represents a mole of A and its associated water of hydration, r represents the moles of water required for complete vapor saturation and s indicates the amount of A which dissolves in the water.

Defining "q" as the solubility of A per mole of water and assuming that partial pressure and mole percent are equivalent at the conditions of interest then:

$$q = \frac{s}{n - r} \qquad (19)$$

$$P\ \text{total} = r\ p_{H_2O} + (1 - s)\ p_A \qquad (20)$$

$$\frac{r}{1 - s} = p_{H_2O}/p_A \qquad (21)$$

Here, p_B and p_{H_2O} refer to the partial pressures of A and water respectively. These equations after re-arranging become:

$$s = q\ (n - p_{H_2O}/p_A)\ /\ (1 - q\ p_{H_2O}/p_A) \qquad (22)$$

$$r = (1 - n\ q)\ p_{H_2O}\ /\ (1 - q\ p_{H_2O}/p_A)\ p_A \qquad (23)$$

Since the following statements are generally true:

$$q\ p_{H_2O}\ /\ p_A \ll 1.0$$

$$p_{H_2O}\ /\ p_A \ll n$$

then

$$s = n\ q \qquad (24)$$

$$r = (1 - n\ q)\ p_{H_2O}/p_A \qquad (25)$$

The number of moles in the vapor phase is given by

$$N = 1 + r - s \qquad (26)$$

with r and s defined by the preceding equations.

The change in enthalpy given by the Clapeyron equation can be expressed in terms of the heat of decomposition and the enthalpy changes accompanying the solution of A and the evaporation

of water. Expressing this relationship in equation form and re-arranging to solve for the heat of decomposition, yields:

$$\Delta h_{\text{decomposition}} = \Delta h - s\,\Delta h_{\text{solution}} - r\,\Delta h_{\text{evaporation}} \qquad (27)$$

Above zero degrees Centigrade, the correction terms must be included. Below zero degrees, the second term on the right hand side of equation (27) may be neglected; the solubility of A in ice being essentially zero.

The Clapeyron equation can be integrated if Δh is assumed to remain constant for a small temperature interval. Expressing the gas volume as a function of temperature and pressure by means of a truncated virial equation of state and integrating, yields:

$$\ln P + BP = - \frac{\Delta h}{NRT} + \text{constant} \qquad (28)$$

In this equation B is the second virial coefficient and R is the gas constant. The moles of vapor, N, in the gas phase is given by equation (26) and must be included to account for the volume change due to evaporation of water and solution of hydrate former. A plot of the left hand side of equation (28) versus 1/T will be linear with a slope of $-\Delta h/NR$. The Δh calculated is an average over the temperature range and will apply

to the temperature at the middle of the range. The Δh at different temperatures can be determined from the following equation:

$$\Delta h = \Delta h_o + \Delta C_p (T - T_o) \tag{29}$$

where ΔC_p is the difference in heat capacities at constant pressure of the products and reactants, Δh_o is the enthalpy change calculated from equation (28) and T_o is the mid-point of the temperature range.

Writing "equations" for the decomposition of hydrate while in equilibrium with water and with ice:

$$A \cdot nH_2O \text{ (solid)} \rightleftharpoons A \text{ (gas)} + nH_2O \text{ (liquid)} - \Delta h_1 \tag{30}$$

$$A \cdot nH_2O \text{ (solid)} \rightleftharpoons A \text{ (gas)} + nH_2O \text{ (ice)} - \Delta h_2 \tag{31}$$

and subtracting, yields:

$$\begin{aligned} nH_2O \text{ (liquid)} - nH_2O \text{ (ice)} &= -\Delta h_1 + \Delta h_2 \\ &= \Delta (\Delta h) \end{aligned} \tag{32}$$

At zero degrees the difference in the heats of decomposition is due to the fusion of n moles of water. Therefore:

$$n = \Delta (\Delta h) / \Delta h_{fusion} \tag{33}$$

The solution of equations (24) through (33) requires a trial and error procedure since the value of n is required to solve equations (24) and (25). The effect of r and s on the determination of $\Delta H_{decomposition}$ is, however, quite small for the great majority of cases, reducing the number of trials to two or possibly three.

It was previously mentioned that one objective of this investigation was the determination of the pressure-temperature phase diagram for the sulfur hexafluoride hydrate. With this data and the preceding equations, the hydrate composition will be calculated and used to determine $\Delta\mu^{II}$ from equation (3b).

D PREDICTION OF INITIAL HYDRATE FORMING CONDITIONS

In 1941 Wilcox, Carson and Katz (35) proposed that gas hydrates could be treated in a manner similar to vapor-liquid equilibria with the mole fraction of a component in the gas phase equaling the product of some empirically determined equilibrium constant K and the mole fraction of the same component in the hydrate on a water free basis. Carson and Katz (1) presented equilibrium constants for methane, ethane, propane and isobutane which were calculated in the following manner. Carson and Katz plotted the equilibrium constants reported by

Hammerschmidt (12) for methane at 600 psia and in a natural gas pipeline, as a function of temperature on semi-logarithmic paper. Using the pressure-temperature equilibrium diagram for pure methane as a starting point on the K = 1 line and one value of K for each of a number of pressures from the methane-propane system, they constructed curves of K versus T for methane at constant pressure approximately parallel to the 600 psia curve. Using these curves as a basis, the equilibrium constants for ethane, propane and isobutane were determined from the ternary systems that each component formed with methane. The prediction of initial hydrate forming conditions in natural gases using this correlation has been fairly successful since a very large portion of the gas phase is methane.

Consider the system methane-ethane-water where methane is represented by the symbol A. Equations (2a,b,c,d), (3a) and (10a,b) describe the thermodynamic behavior of this system which crystallizes in Structure I with methane entering both cavities and ethane occupying only the larger cavity. Equilibrium constants are given by

$$K = x/y' \tag{34}$$

where x is the mole fraction in the gas phase and y' the mole

fraction in the hydrate on a water free basis. The relationship between y and y' is given by:

$$y_A' = (v_1 y_{A1} + v_2 y_{A2}) \;/\; (v_1 y_{A1} + v_2 y_{A2} + v_1 y_{B1} + v_2 y_{B2}) \qquad (35)$$

From equation (2a,b,c,d) the y values are determined by the partial pressures and C values for each component. It must be noted that y_{Ai} is a function not only of the physical constants for A but also of the constants of the other component. In other words the value of y_A' is valid only for the system for which it was determined and will vary from system to system. Furthermore, K values calculated for systems crystalizing in Structure I are obviously not valid for a system which crystallizes in Structure II. Not only do the other components have an effect but the constants for methane are not the same since the geometry of the cavities occupied by methane is certainly different. To determine the effect that different molecules have on the equilibrium constants for methane, the pressure-composition diagram of the methane-sulfur hexafluoride hydrate at -3 degrees Centigrade will be used to calculate the K values of methane. These values will be compared with the methane equilibrium constants calculated from Figure VIII and with the K charts for methane presented by Katz et al (15).

EXPERIMENTAL

A EXPERIMENTAL EQUIPMENT

The experimental apparatus used in this work was similar to that used by Otto (21) and Snell (27) in their studies on hydrates. The assembly consisted essentially of a continuously agitated equilibrium cell where the hydrate was formed, an auxiliary cell for measuring the quantity of gas introduced to the equilibrium cell and measuring devices to determine the pressure and temperature in both cells. Figure X is a schematic diagram of the equipment and piping arrangements and Figure XI shows the assembled apparatus.

1 The Equilibrium Cell

The equilibrium cell was the cell used by Snell for his low pressure studies on the hydrate system methane-ethylene-propylene-water. This cell, which is shown in Figure XII, was a Jerguson liquid level gauge, constructed from type 304 stainless steel and was capable of withstanding 2000 psi at 100 degrees Fahrenheit. Two sightglasses, on front and back, ran the full length of the cell making the contents readily

FIGURE X

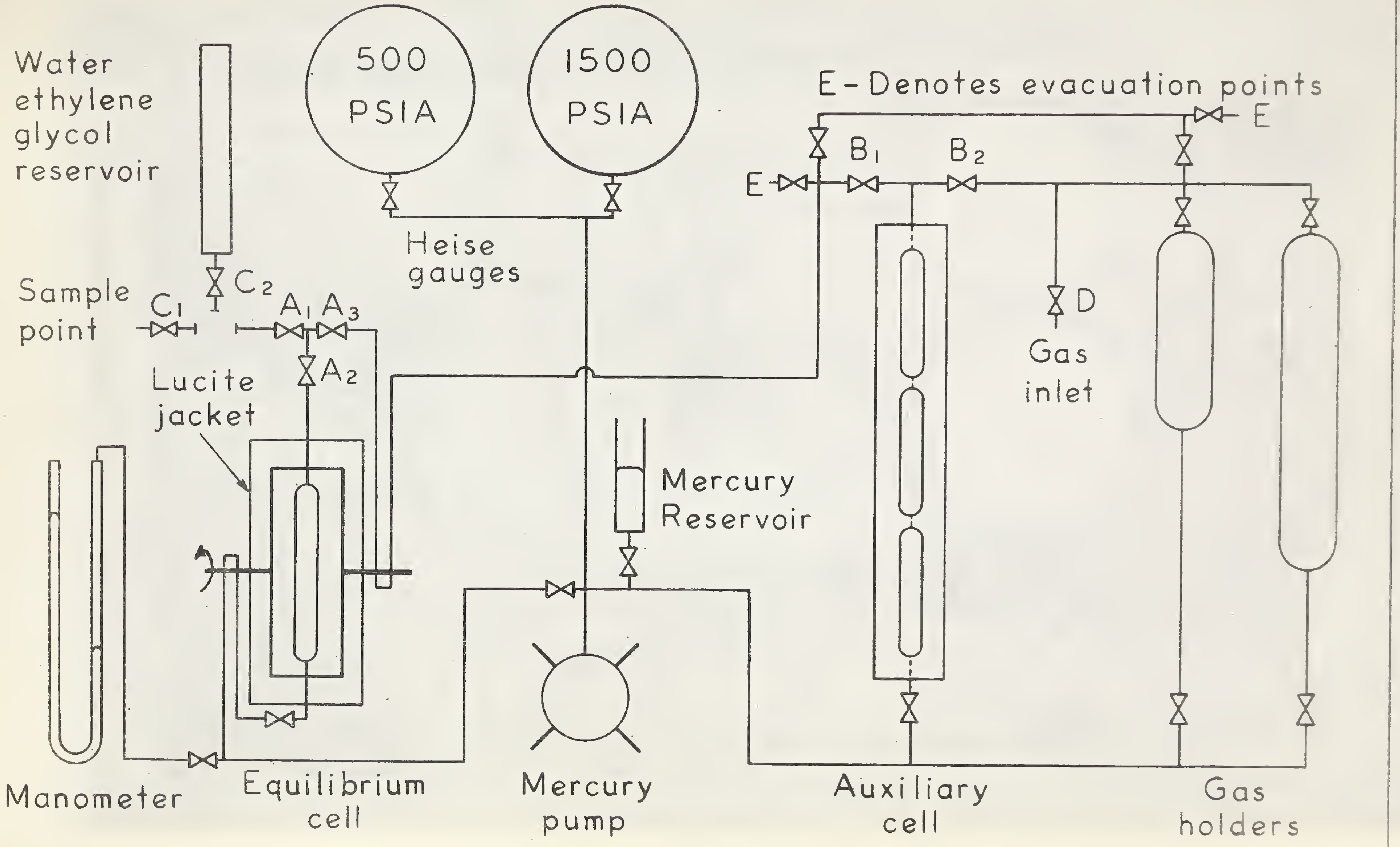

Schematic Diagram of Equipment

FIGURE XI

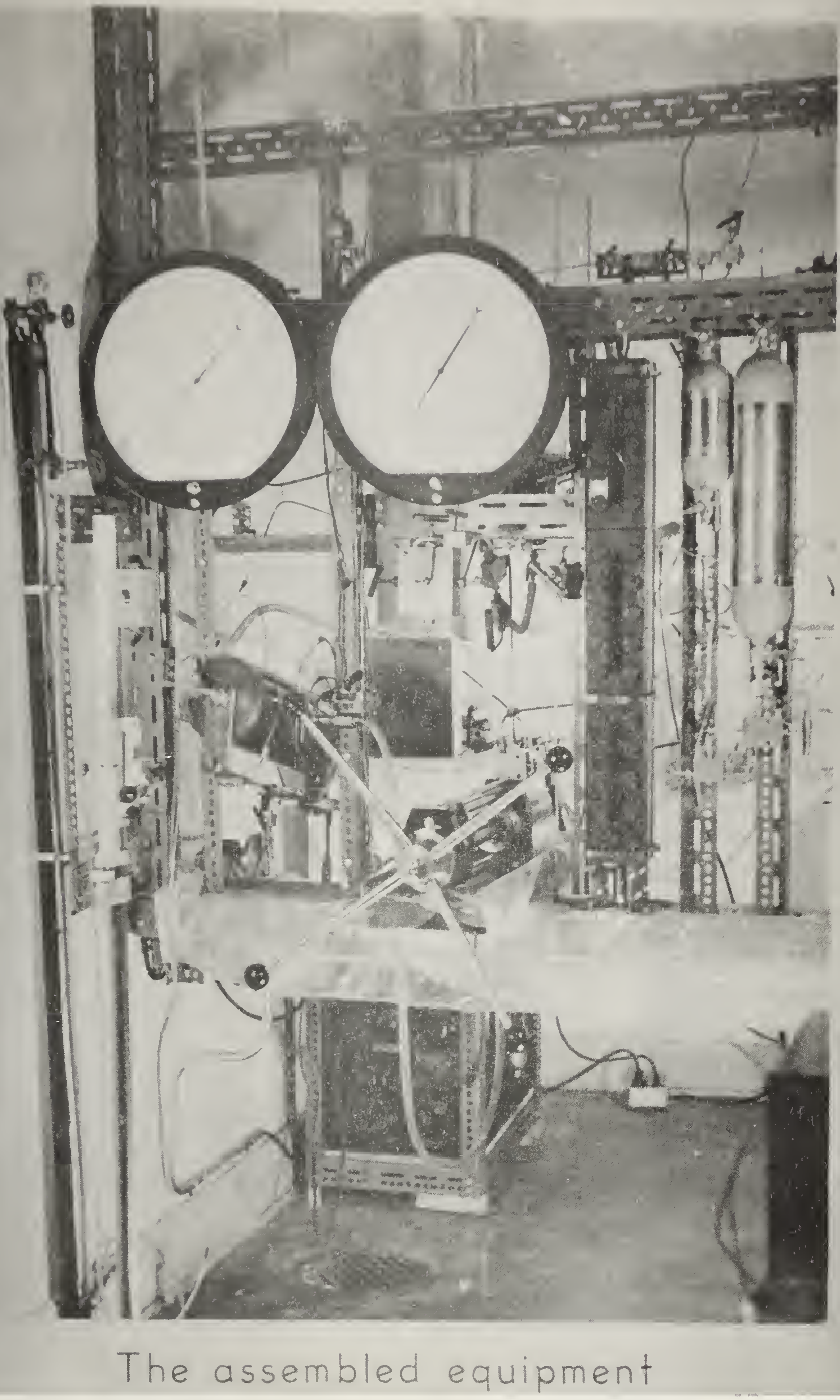

The assembled equipment

FIGURE XII

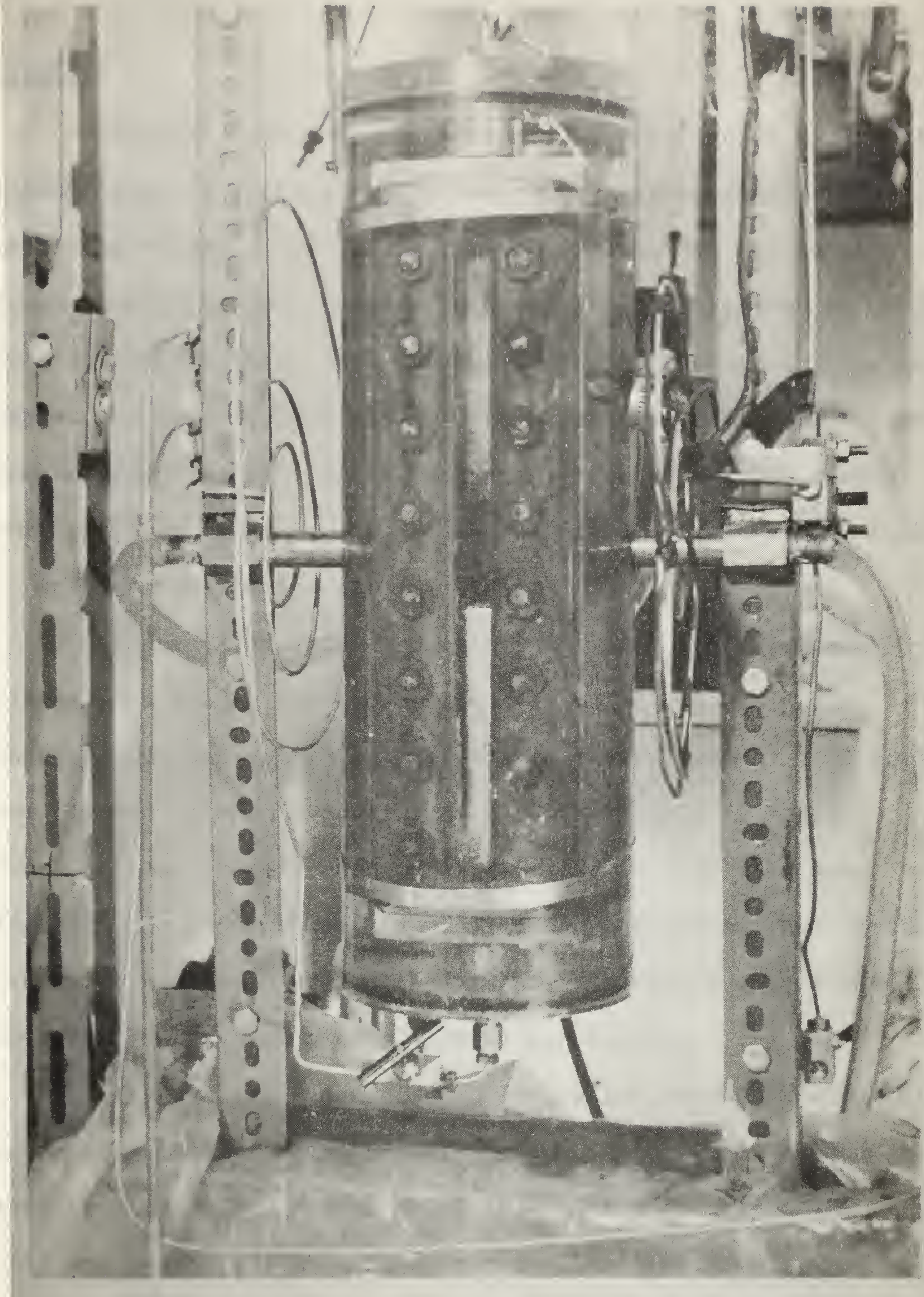

The Equilibrium Cell

visible.

The cell was enclosed in a cylindrical jacket of lucite through which a cooling medium was circulated to regulate the cell temperature. The cell was pivoted about its centre on trunions with conical bearing surfaces for the trunions machined into the cell walls. The trunions projected through the lucite jacket and were rigidly held by the supporting framework allowing no weight to rest upon the lucite. Except for the bearing surfaces, the trunions were hollow, permitting passage of coolant to and from the lucite case.

Figure XIII shows the agitation mechanism which consisted of a 1/12th horsepower electric motor connected via an eccentric and connecting rod to the lucite jacket. The cell was pivoted through a small arc of approximately 25 degrees about the horizontal causing the contents to move back and forth in the cell thereby furnishing the agitation. The vertical travel by one end of the cell was approximately 4 inches with an agitation frequency of 57 cycles per minute.

The cell was connected to the system through two spiral coils of Autoclave high pressure tubing, with one coil about each trunion (cf. Figure XII). This method of connecting cell and system was particularly convenient for the type of

FIGURE XIII

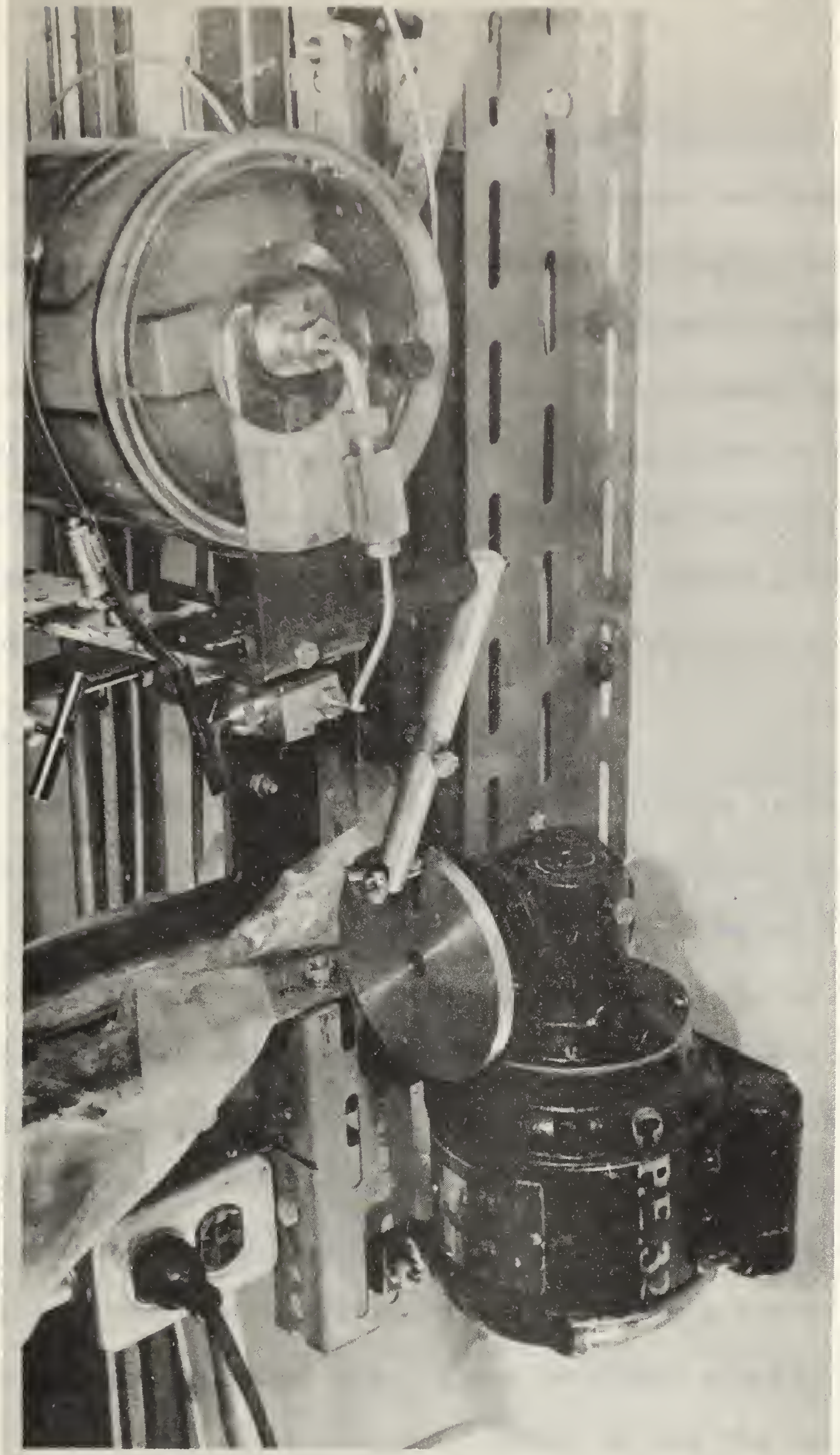

The Agitation Mechanism

agitation used and proved both flexible and trouble-free.

A volumetric calibration of the cell was required to determine the amount of vapor phase present following the establishment of equilibrium. A calibration of volume in terms of height accurate to ±0.2 cubic centemeters was obtained for this cell. The calibration is included in the Appendix where the gas phase volume is plotted as a function of height with the volume of the tubing leading to valve A_2, Figure X being included as part of the cell volume.

2 Control and Measurement of Temperature

The temperature of the equilibrium cell was controlled by circulating a coolant from an auxiliary temperature bath through the lucite jacket surrounding the cell. Marcol 20, a product of Imperial Oil Limited, was first used as the cooling medium but was unsuitable because it formed a stable emulsion with water. This emulsion could not be removed by a rock salt filter incorporated in the re-circulation line and the substitution of a more deliquescent material, calcium chloride, for rock salt was not satisfactory due to the very marked rate that the carbon steel sight glass retainers started to corrode. A further disadvantage of Marcol 20 was the precipitation of a waxy material upon the windows and lucite walls.

The combination of water emulsion and precipitate rendered the contents of the cell completely indistinguishable. Using varsol as a temperature medium overcame the two main disadvantages of Marcol 20. In addition, the lower viscosity increased heat transfer, thereby decreasing the time required to change the bath temperature.

The auxiliary bath consisted of an insulated tank with an immersion pump for circulating the coolant. A Freon refrigeration unit with coils immersed in the bath, cooled the fluid while a 500 watt immersion heater was used for heating purposes. The temperature was controlled by an American Instrument Company bi-metallic strip controller which could be used to govern either the refrigerator or the heater but not both. A one minute delay relay was incorporated in the control circuit to decrease the reaction time of the controller. While the bath temperature could be maintained to only plus or minus 0.25 degrees Centigrade, the cell temperature fluctuated very little, less than plus or minus 0.05 degrees, due to its large heat capacity.

The temperature of both cells was measured with iron-constantan thermocouples and a Leeds-Northrup Model K-2 potentiometer. These thermocouples were calibrated to plus or minus

0.02 degrees Centigrade by the Standards Laboratory of the Chemical and Petroleum Engineering Department of the University of Alberta. A platinum resistance thermometer standardized by the United States National Bureau of Standards, and a Leeds-Northrup Meuller Bridge were used to determine accurately the temperatures for the calibration while e.m.f. was measured on a Leeds-Northrup Model K-3 potentiometer. The calibration curves are included in the Appendix.

The hot junction of the equilibrium cell thermocouple projected through the cell wall into the interior, measuring the temperature of the contents directly. A pressure tight seal was achieved by silver soldering the hot junction into a short section of Aminco tubing connected to the cell by an Aminco male connecter. The thermocouple to the auxiliary cell rested in a well in the cell wall and measured the body temperature only. The cell and contents were allowed to attain thermal equilibrium before a measurement was made.

3 Measurement of Pressure

A range of pressures from 6 psia to 1500 psia was measured. Three measuring devices were used, a water over mercury manometer, a 500 psig Heise bourdon tube gauge and a

1500 psig Heise bourdon tube gauge. The Heise gauges were calibrated in situ to plus or minus 0.1 and 0.2 psig respectively using a Ruska Instrument Corporation Dead Weight Tester. The zero points of the gauges, initially set with the dead weight tester, were periodically checked with the manometer but little deviation with time occurred. The reference level on the dead weight tester denoting zero psig was transferred to the framework supporting the experimental equipment and became the point to which all measurements of pressure and volume were referred. Corrections for atmospherical pressure and the head of mercury between cell and reference level were made for all pressure measurements.

The cells were pressurized by injecting mercury into the bottom of the cells with a Ruska Instrument Corporation positive displacement pump. The volumetric scale on the pump was calibrated by weighting the quantity of mercury displaced from the pump and was the standard for the cell volume calibrations.

4 Equipment - General

(a) Valves and Tubing

Two types of tubing and fittings were used in the experimental apparatus, Aminco and Autoclave. The Aminco tubing

was suplied by the American Instrument Company, Inc. and had an inside diameter of 3/32 of an inch with 1/8 inch walls. Both tubing and fittings were constructed of type 304 stainless steel and rated for 30,000 psi at 100 degrees Fahrenheit. The Autoclave tubing, made by Autoclave Engineers, Inc. had an outside diameter of 1/8 of an inch with a wall thickness of 1/32 of an inch. The tubing and valves were rated for 15,000 psi at 100 degrees Fahrenheit and were constructed of type 316 stainless steel. The Autoclave tubing was of lighter construction and was much the easier to manipulate. Difficulty arose during equipment evacuation due to the time required to attain the desired vacuum via the small tubing. Several evacuation points were provided to circumvent this difficulty by reducing the amount of line through which the equipment was evacuated. Evacuation was accomplished by a General Electric duo seal vacuum pump with the resulting vacuum being measured with a MacLeod gauge.

(b) Auxiliary Cell

The volume of gas admitted to the equilibrium cell was measured in an auxiliary cell. This cell, a Jerguson liquid level gauge, was rated for 3000 psi at 100 degrees Fahrenheit and contained two glass windows, front and back, which ran the

full length of the cell allowing the contents to be readily visible. The volume calibration of this cell was performed in the same manner as the equilibrium cell calibration. The Appendix contains the calibration curve in which the volume of the cell is plotted as a function of height. The volume of the tubing leading from the top of the cell to the nearest valves was included with that of the cell. The accuracy of the calibration was plus or minus 0.2 cubic centimeters.

(c) Mercury Cleaning

The mercury in the auxiliary cell formed a scum which adhered to the glass windows obscuring vision. This scum formed only when air was present and was similar in appearance to that formed on mercury from a mercury Oxifier. Apparently trace impurities picked up by the mercury from the equipment was oxidized.

The mercury used in the equipment was cleaned in the following manner. The dirty mercury was first filtered through a paper filter to eliminate macroscopic debris followed by oxidation of impurities in a Mercury Oxifier manufactured by the Bethlehem Instrument Company. The mercury from the Oxifier was filtered in a Bethlehem Instrument Company Type F mercury filter operating on the gold leaf adhesion principle. Distillation in a Central Scientific Company mercury distillation unit completed

the purification procedure.

(d) Gas Purification

The sulfur hexafluoride was obtained from Matheson of Canada Ltd. and contained air as the only detectable impurity. Removal of the air was accomplished by subliming the impure gas into a closed glass bomb immersed in a dry ice-acetone bath and evacuating the air with a vacuum pump. The apparatus is shown in Figure XIV. Most of the air was removed directly while the remainder was flushed out in a flow of sulfur hexafluoride vapors from the sublimed solid. Evacuation continued until the vapors contained a negligible amount of air. The dry ice-acetone bath maintained the temperature approximately nine degrees below the sublimation temperature of sulfur hexafluoride. The purified gas was stored in the gas holders shown in Figure X and analysis of the final product indicated that the gas purity was slightly greater than 99.7%.

The methane was obtained from the Phillips Petroleum Company with a specified purity of 99.8%. Analysis of the gas showed that the specifications had been met and no additional purification was attempted.

FIGURE XIV

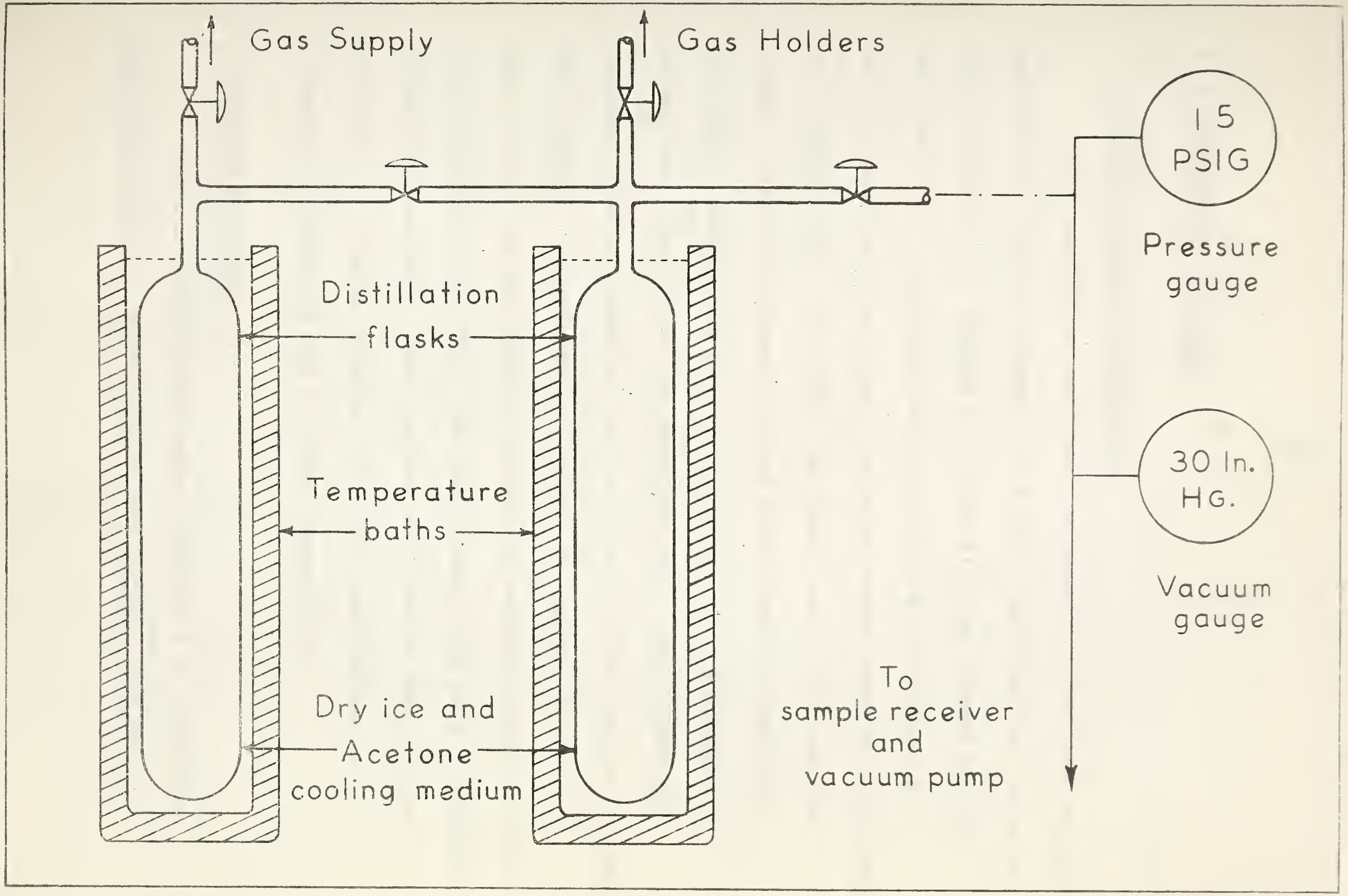

Gas Purification Apparatus

B EXPERIMENTAL TECHNIQUE

1 Charging the Equilibrium Cell

The equilibrium cell was fastened in a vertical position and mercury injected through the bottom expelling the contents through valve A(1), Figure X. Valve A(2) was closed and the contents of the auxiliary cell were forced out through A(1) and the water-ethylene glycol solution drawn into the equilibrium cell through A(1), A(2) with the Ruska pump. A(1) was then closed. The line between the gas holder and the auxiliary cell was evacuated and gas, to a predetermined pressure and volume, was admitted to the auxiliary cell from either the methane cylinder connected to D or directly from the gas holders. The pressure, temperature and volume of the gas in the cell were noted. The gas was then forced by mercury injection into the equilibrium cell until the connecting lines were completely filled with mercury. More gas was admitted to the auxiliary cell and the process repeated until the equilibrium cell contained a charge of the required composition.

2 Hydrate Formation

Hydrates were formed under three sets of conditions requiring different approaches to the initial formation of

the hydrate crystals.

(a) The Binary System S F_6 - H_2O Above Zero Degrees Centigrade

The three phase equilibrium, hydrate-aqueous liquid-gas, was determined above zero degrees Centigrade. An application of the Phase Rule reveals that the equilibrium is univariant with an unique pressure for each temperature. The procedure followed was to set the temperature to some value and increase the cell pressure well above the equilibrium value until hydrate started to form. A pressure decrease indicated initial hydrate formation. The pressure was decreased to a point approximately 20 per cent above the estimated equilibrium value and the cell agitated until equilibrium was achieved. The values of pressure and temperature were recorded before the hydrate was decomposed and the cell made ready for the next determination. The time required for equilibrium to be established was approximately eight hours.

Approximately 20 cubic centimeters of distilled water was introduced into the cell as described previously. This was sufficient to provide an excess after hydrate was formed.

(b) The Binary System SF_6- H_2O Below Zero Degrees Centigrade

In this region, the three phases in equilibrium are

hydrate, ice and gas. The equilibrium is univariant and is an extension of the HL_2G line of section (a) with ice replacing aqueous liquid as the third phase. Since diffusion in the solid phase is very slow, an auxiliary solvent was added to speed the establishment of equilibrium. If the molecules of the solvent are too large to fit into the cavities of the hydrate, the additional phase will have no effect upon the composition of the solid. Provided the solvent has a low vapor pressure, the partial pressure of the solutes in the gas phase will not be affected. The only result of adding the solvent will be to "catalyze" the reaction. Ethylene glycol was employed following the satisfactory use of this solvent by Platteeuw and van der Waals (20) in their hydrate studies.

An aqueous solution of ethylene glycol was so prepared that under the experimental temperature chosen, 30 cubic centimeters of solution would yield approximately 15 cubic centimeters of ice. The glycol solution, inserted into the cell according to the procedure previously outlined was followed by approximately 30 cubic centimeters of gas at a pressure close to the range of interest. The pressure was lowered as far as possible by removing mercury from the cell and ice was formed

by subcooling the cell. Following ice formation the temperature was adjusted to the desired value and the pressure increased to a point where hydrate commenced to form. The pressure was then lowered to approximately 20 per cent above the estimated equilibrium value and the cell agitated until equilibrium was achieved; usually a period of 24 hours was required. Pressure and temperature of the cell contents were recorded before the hydrate and ice were decomposed in preparation for another run.

Formation of ice prior to that of hydrate was required because an equilibrium was established between hydrate, gas and glycol solution in the absence of ice. The pressure for this equilibrium was below that for hydrate, gas and ice and led to erroneous results. A further discussion of this phenomenon is presented later.

(c) The Ternary System, CH_4-SF_6-H_2O at -3 Degrees Centigrade

The pressure-composition phase diagram on a water-free basis was determined for the system methane-sulfur hexafluoride-water at -3 degrees Centigrade. The construction of the diagram required a knowledge of the compositions of the gas and hydrate phases in equilibrium with each other at various total pressures. The gas phase composition was determined

directly by chromatographic analysis while the composition of the hydrate was calculated from a material balance upon the quantities of gases entering the equilibrium cell and the amount of gas in the vapor phase following the establishment of equilibrium.

The volume, pressure and temperature of the gaseous materials entering the equilibrium cell were determined in the auxiliary cell prior to injection. Since it was desired that approximately half of the gas admitted should form hydrate, a rough material balance determined the quantity of gases to be used. The gases were thoroughly mixed and returned to the auxiliary cell leaving the equilibrium cell at a low pressure in preparation for ice formation. The gas phase volume of the equilibrium cell was adjusted by removing mercury until approximately 70 to 80 cubic centimeters of gas phase existed above the water-ethylene glycol solution. The cell was isolated from the mercury injection system and the gas volume determined. The agitation mechanism was engaged during the sub-cooling stage required for ice formation and the subsequent temperature adjustment to -3 degrees Centigrade. The volume of gas contained by the auxiliary cell was injected by mercury displacement until the first drop of mercury appeared

from the connecting lines. The cell was isolated from the system by closing valves A2, A3 and agitation begun. After the cell volume was determined, the quantity of mercury in the cell was not altered. The volume change caused by the formation of a few grams of ice was neglected and it was assumed that the volume did not change during hydrate formation.

A period of one to two days was allowed for equilibrium to be established before final pressure and temperature readings were taken and the gas phase analyzed. The sample to be analyzed was transferred isothermally and isobarically to an evacuated sampling receiver connected to valve A1 and then analyzed by gas-liquid partition chromatography.

The experimental pressure was below atmospheric for one of the runs requiring a modification of the sampling technique. The lines between the equilibrium and auxiliary cells were cleared of mercury by injecting air through valves A1, A3, B and into the auxiliary cell. The lines and cell were evacuated before the gas phase was transferred isobarically to the auxiliary cell. The gas pressure in the cell was increased by mercury injection allowing a sample to be taken.

A direct check upon the hydrate composition was performed for some of the runs by removing, isobarically, all of the gas phase, decomposing the hydrate and analysing the resulting vapors. Occlusion of some gas in the cell during the vapor phase removal resulted in a slightly high methane concentration; however, the check was within one or two per cent.

3 Chromatographic Analysis

All of the gases were analyzed using gas-liquid partition chromatography. A Kromo-Tog, model K-2 manufactured by the Burrel Corporation was used with a one meter silica gel column for all analyses. A helium flow rate of 15 milliliters per minute with the column at room temperature, split the sample cleanly into its various parts with no overlapping of components. The resulting peak heights were used as a measure of the quantity of each component present, thereby requiring the analysis of samples of known composition and preparation of per cent component versus peak height charts. Such charts, constructed for methane and sulfur hexafluoride mixtures, are included in the Appendix.

The samples used in the calibration were prepared in a 100 milliliter gas burette with the equivalence of mole

per cent and volume per cent being assumed. Due to the marked difference in molecular weights of the two gases, complete mixing was assured by passing the gases back and forth through a short, fine capillary until uniformity was achieved.

Since peak heights vary with column temperature, the total per cent of each sample was adjusted to 100 by increasing or decreasing the per cent of each component by an amount proportional to the value indicated by the charts. This correction was found in the literature and verified by Snell (23).

EXPERIMENTAL RESULTS

A THE BINARY SYSTEM SULFUR HEXAFLUORIDE-WATER

Pressure-temperature equilibria were determined for the gas hydrate of sulfur hexafluoride for pressures ranging from 7.90 to 219.0 psia and temperatures from -8.14 to 12.84 degrees Centigrade. The pressure-temperature data are presented in graphical form in Figure XV and in tabular form in Table I of the Appendix. The vapor pressure curve for pure SF_6 (17) is included on the Figure.

The quadruple point $H_{II}L_1L_2G$ will be close to the intersection B of the vapor pressure curve and the extrapolated $H_{II}L_2G$ line. Point B represents a temperature of 13.7 degrees Centigrade and a pressure of 268 psia. The intersection of the equilibria $H_{II}IG$ and $H_{II}L_2G$ will be at zero degrees Centigrade since the shift of the freezing point of water due to gas solubility is negligible for this system. The slight effect that pressure exerts on the freezing point of water was neglected in the construction of $H_{II}L_2I$.

Above zero degrees Centigrade, the pressure-temperature phase diagram exhibited behavior similar to diagrams reported

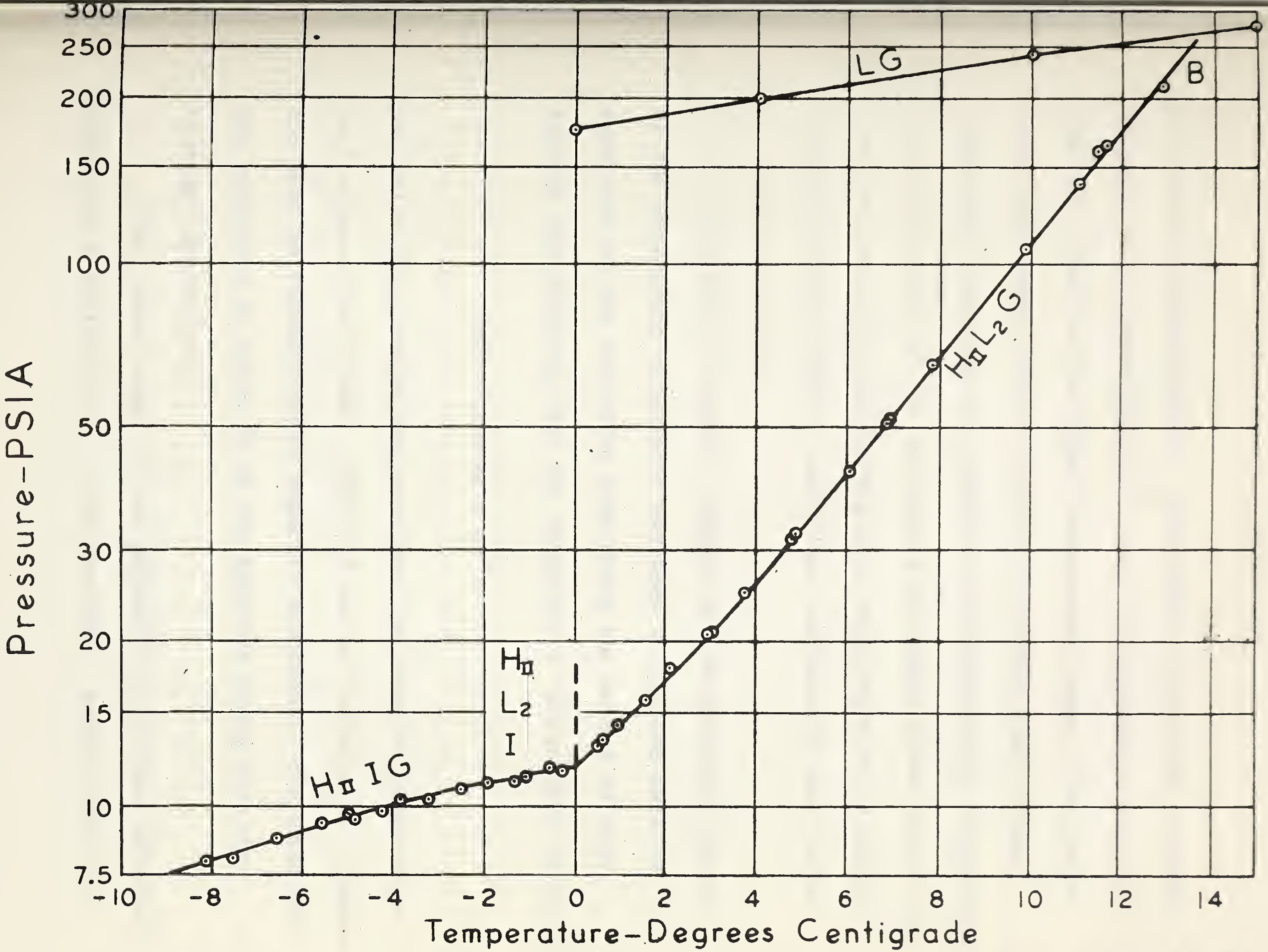

Pressure-temperature phase diagram for system SF_6-H_2O

for other hydrate systems. The slope of the curve increased slightly with temperature near zero and attained a fairly constant value in the higher temperature range. The curve below zero showed similar behavior with the slope being shallowest near zero and increased with decreasing temperature. The intersection of the two curves was quite close indicating that the use of the ethylene glycol had little or no effect upon the hydrate forming conditions and hence it was present as a "catalyst" only.

The LGP 30 digital computer at the Computing Centre of the University of Alberta was used to fit the data to equations of the following form using the method of least squares and assuming that the temperature values were correct.

$$\ln P = A + Bt + Ct^2 + \ldots$$

The units of pressure were psia and the units of temperature were degrees Centigrade. The data are in two separate regions and must be represented by separate equations. The equations are contained in Table IV of the Appendix along with the standard deviations.

The lowest order of the polynomial in "t" was selected that gave a satisfactory fit of the data. Because the two

curves must intersect at zero degrees Centigrade, the difference between the two equations at zero was used as a second criterion of acceptability. For these reasons the quadratic equation was selected for the data below zero and the cubic above zero. The chosen equations yield values at zero of 11.84 and 11.82 psia for the data below and above zero respectively.

An eight degree temperature interval of the pressure-temperature equilibrium diagram was used to determine the hydrate composition at zero degrees Centigrade. This interval contained sixteen data points, eight above and eight below zero. The left hand side of equation (28) was calculated using the experimental data points and was plotted as a function of 1/T. Two plots were necessary, one below zero and the other above. By the method of least squares, a linear equation was determined to represent the plotted data and Δh was calculated from the slope of the equation. The experimental data were estimated to be accurate to plus or minus 0.1 degrees Centigrade and to plus or minus 0.05 psi below zero and to plus or minus 0.1 psi above. The ratio of the effects that these possible errors in temperature and pressure had upon the slope of equation (28) was determined and used as a weighting factor

in the least square calculations. For the data below zero, it was determined that the effect of the possible error in pressure was approximately 1.3 times as great as the effect of a possible temperature error. Above zero, this ratio was 0.35.

The equations from which the coefficients of the linear equations were calculated, are presented in Table V. From these linear equations, calculated by least squares, the Δh's were calculated for the temperature interval above and below zero. The mid-points of these temperature intervals were +1.86 and -1.90 degrees Centigrade. The Δh's were determined at zero degrees using equation (29) before corrections for gas solubility and for evaporation of water were made. These calculations are summarized in Table VI.

The corrected values of Δh calculated at zero degrees are -5,137 calories per gram mole for the formation of hydrate from ice and -29,569 calories per gram mole for the formation of hydrate from water. From equation (33), the number of water molecules associated with each molecule of sulfur hexafluoride in the hydrate at zero degrees Centigrade is 17.02 plus or minus 0.1. Using this value, $\Delta\mu^{II}$ was calculated from equation (3b) to be 211 calories per gram mole of water.

B THE TERNARY SYSTEM SULFUR HEXAFLUORIDE-METHANE-WATER AT -3°C

The pressure-composition diagram was determined for the gas hydrate of sulfur hexafluoride-methane on a water free basis at -3 degrees Centigrade. The data are presented in Figure XVI where the small circles represent experimental points and the curve represents the theoretical prediction. The similarity between Figures VIII and XVI is evident and to facilitate comparison, the data are plotted in a similar fashion.

The hydrate composition was determined by a material balance on the quantities of gases entering the equilibrium cell and the amount and composition of gas in the final vapor phase. The virial equation of state with the second virial coefficient was used to calculate the number of moles of gas present. The second virial coefficients for the pure gases, sulfur hexafluoride and methane, were taken from Clegg (3) and Mueller (18) respectively while the second combinatorial coefficient for sulfur hexafluoride-methane mixtures was taken from Hammond et al (13).

Van der Waals and Platteeuw (33) have reported a value of 570 atmosphere^{-1} for C_2 of sulfur hexafluoride and

FIGURE XVI

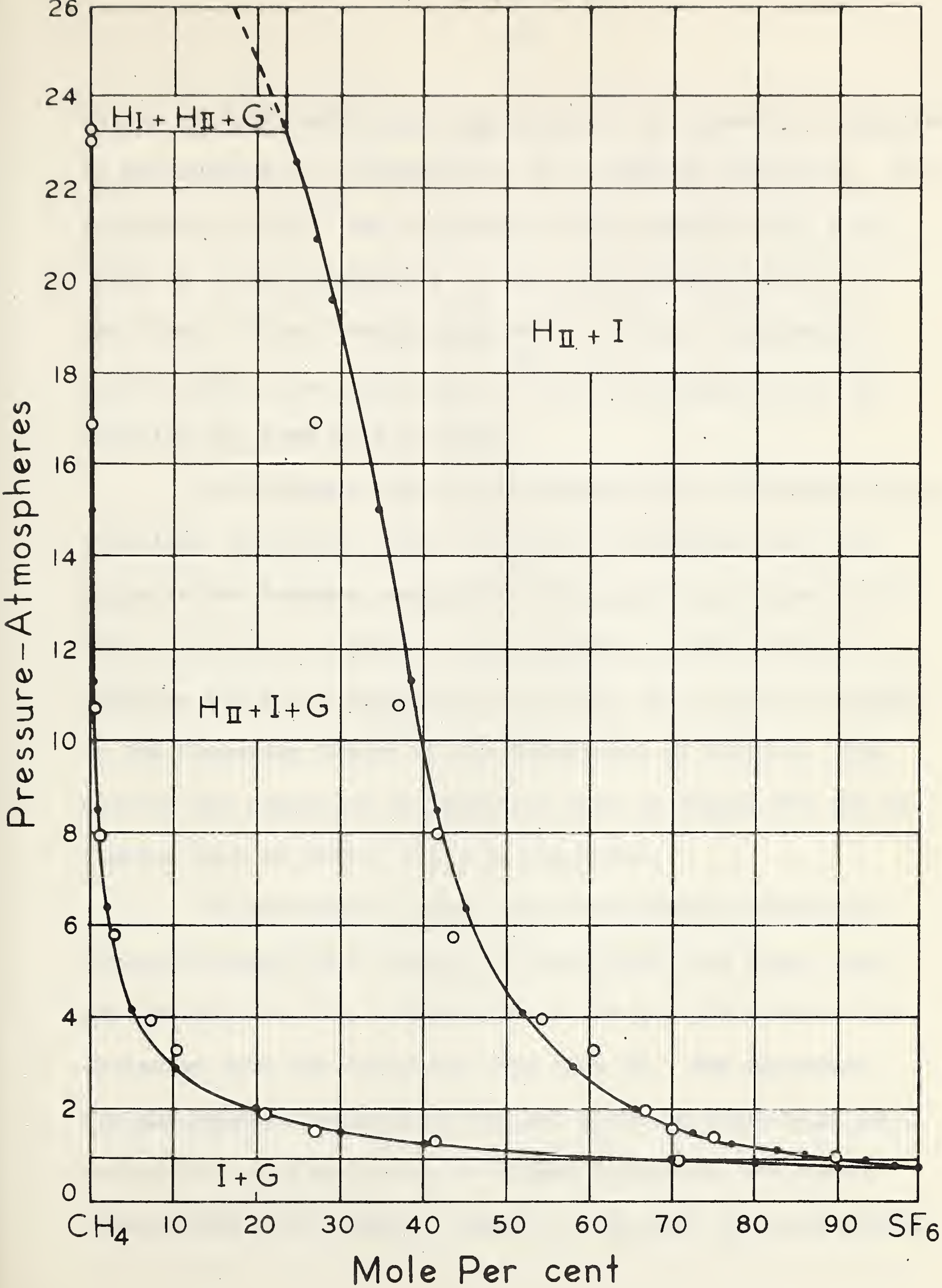

Isothermal cross-section of the system CH_4-SF_6-H_2O on a water-free basis at -3° C.

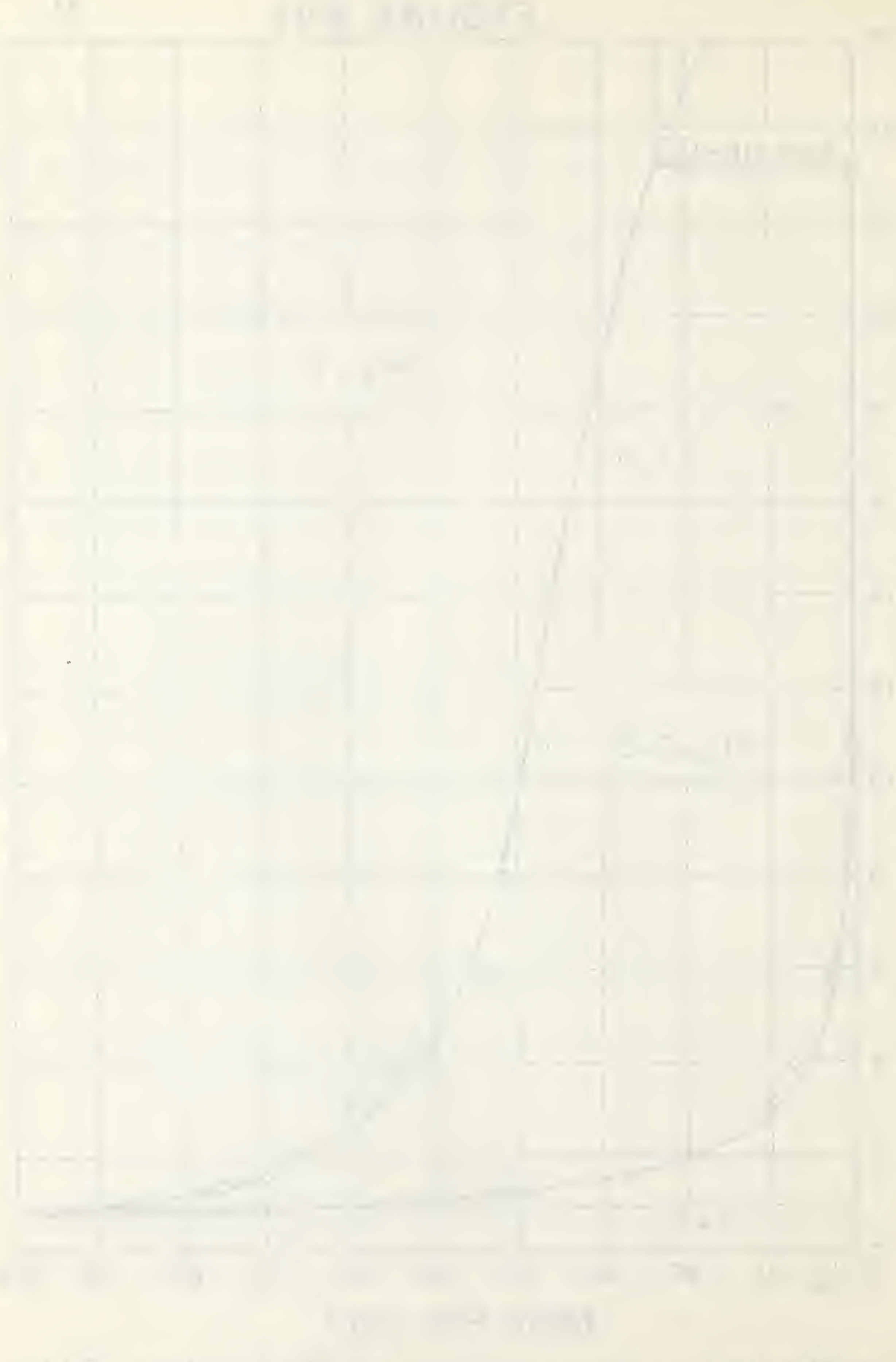

[illegible]

[illegible]

values of 0.212 and 0.161 atmospheres^{-1} for C_1 and C_2 respectively for methane at a temperature of -3 degrees Centigrade. For Structure II, $\Delta\mu^{II}$ was calculated using equation (3b) and a value of 0.716 atmospheres for the equilibrium pressure of the binary sulfur hexafluoride-water system as determined in this work. The value of $\Delta\mu^{II}$ was determined to be 190 calories per gram mole of water.

The pressure-composition diagram was constructed using equations (2a,b,c,d), (12) and (13) to determine the total pressure and hydrate composition for various gas compositions. The calculation of these values required a trial and error solution which was performed by the IBM 1620 digital computer at the Computing Centre of the University of Alberta. The results are presented in graphical form in Figure XVI and in tabular form in Table III of the Appendix.

The agreement between the theoretically predicted pressure-composition diagram and experiment was quite good, particularly for the composition of the gas phase where the deviation from the curve was less than 2%. The agreement for the hydrate composition was not quite as close with the deviations occuring mainly at higher pressures, but in no instance were they greater than 5%. The data for this branch

of the diagram are not randomly scattered about the theoretical but appear to have a trend with a larger sulfur hexafluoride fraction at lower pressures and a larger methane fraction at higher pressures. This indicates that either a slight adjustment of the values for the C_{Ki} is required to shift the predicted curve onto the experimental data or that equilibrium was not attained in the hydrate phase. The attainment of equilibrium in the hydrate depended upon diffusion in the solid phase which was very slow unless some means was provided to accelerate the equilibrating process. In this case the presence of an auxiliary phase containing ethylene glycol provided the mechanism by which the rate was increased. The glycol solution was maintained in intimate contact with the hydrate and, although at least 24 to 48 hours were allowed for the equilibrium to be established, there may have been some crystals of hydrate which had not reached equilibrium. However, an increase in the length of time allowed for the equilibrium process to take place did not appreciably alter the results.

C EQUILIBRIUM CONSTANTS FOR SULFUR HEXAFLUORIDE AND METHANE AT -3°C

The equilibrium constants for methane and sulfur hexafluoride were calculated using equation (34) and the pressure-

composition phase diagram for the system sulfur hexafluoride-methane-water at -3 degrees Centigrade. The calculated values are contained in Figures XVII and XVIII together with equilibrium constants from the pressure-composition phase diagram determined by van der Waals and Platteeuw (33) for the methane-propane-water system, and from the charts of equilibrium constants contained in Katz et al (15). The curves are from the theoretical prediction of the pressure-temperature diagram for the sulfur hexafluoride-methane-water system and the points are from the experimental data.

The equilibrium constants determined for methane from the experimental results of this work and from van der Waals and Platteeuw are in the same range but are not coincident. The most deviation appears at low pressures where they differ by approximately 15%. As the pressure increases, the deviation becomes smaller and the values become quite close together. That the constants from the two different systems are in the same range is not surprising since the C_{Ki} for methane are three orders of magnitude smaller than the values for either sulfur hexafluoride or propane while these differ by a factor less than two. The equilibrium constants from the charts in Katz et al are in poor agreement with the experimental

FIGURE XVII

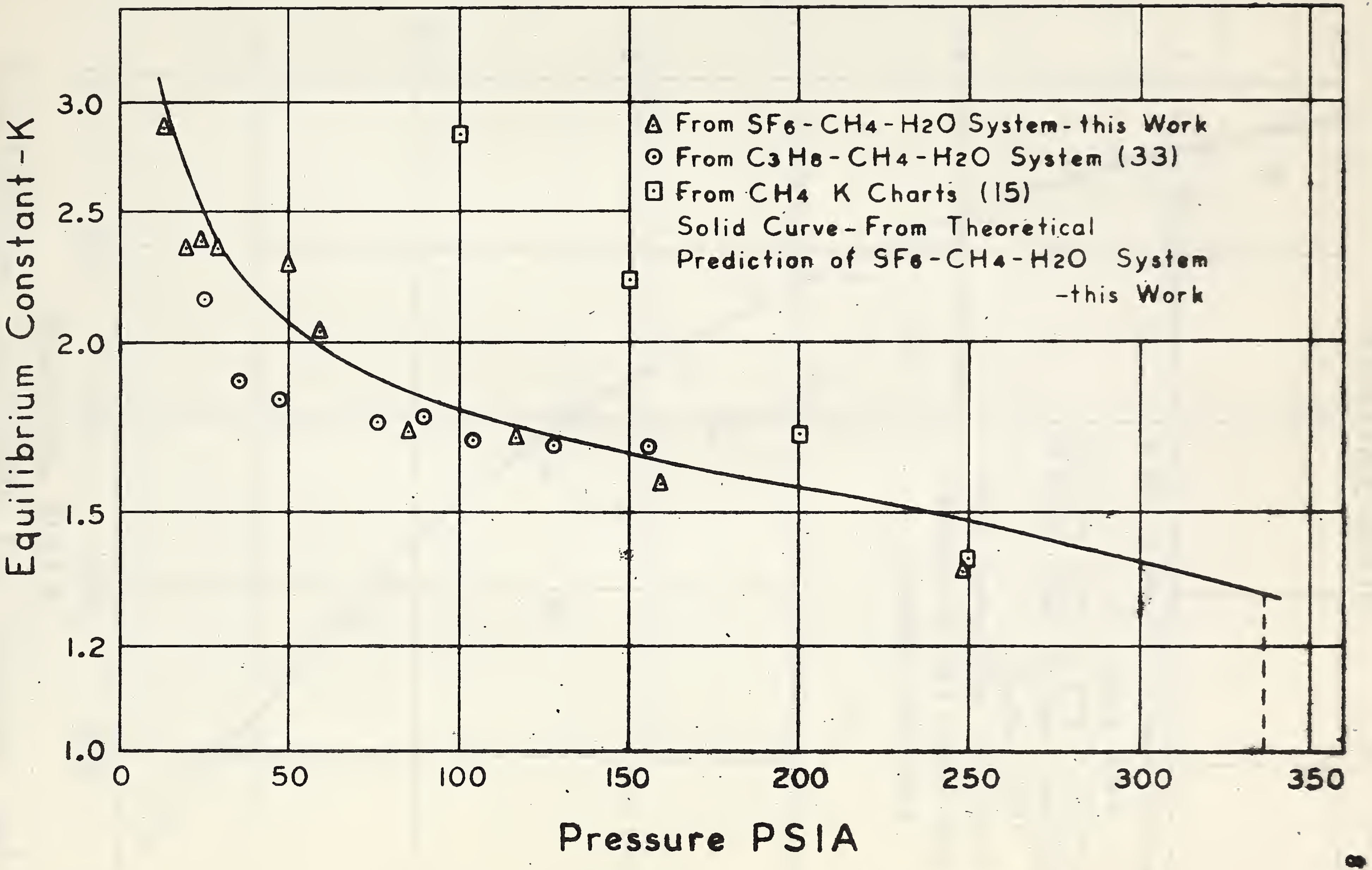

Equilibrium Constants for Methane at -3°C

FIGURE XVIII

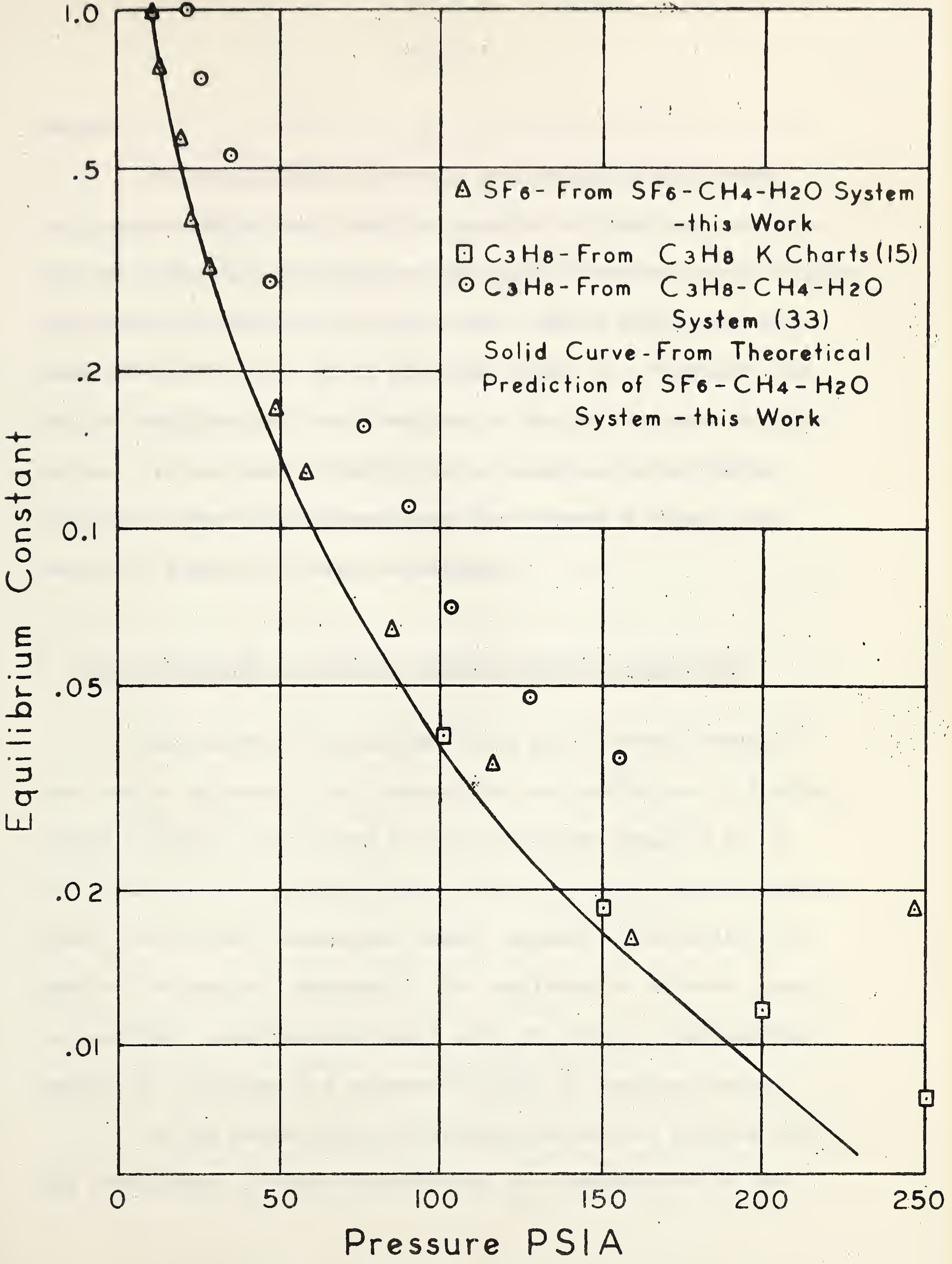

Equilibrium Constants for Propane and Sulfur Hexafluoride at −3°C

values.

The equilibrium constants for sulfur hexafluoride and propane calculated from the results of this work and from van der Waals and Platteeuw respectively form two smooth curves approximately parallel to each other. The K values for propane taken from Katz et al are much closer to the values for sulfur hexafluoride than they are to the experimental propane values. Errors are probably due to incorrect equilibrium constants taken for methane when the propane K charts presented in Katz et al were calculated.

D THE PREDICTION OF INITIAL HYDRATE FORMING CONDITIONS

The empirical technique using equilibrium constants has been a valuable first attempt in the prediction of initial hydrate forming conditions by the petroleum industry but a more theoretical approach would have more general application. Since statistical mechanical theory appears to describe the physical situation adequately, the application of this theory to practical calculations would seem in order. One possible method of utilizing the proposed theory is outlined below.

In the method for predicting the initial hydrate forming conditions, it was assumed that the composition of the

gaseous phase was known, that the total pressure of the system was fixed and that the temperature for the initial hydrate formation was the required unknown. The proposed method for determining the temperature requires that tables for each hydrate structure listing $\Delta\mu$ and the values of C_{Ki} for each hydrate former as functions of temperature be compiled. Once the gas composition and pressure were known, the determination of the initial hydrate forming temperature would require the solution of a series of equations for y_{Ki}, the fraction of each type of cavity filled with each molecular species. These equations are applications of equation (2) with values of C_{Ki} taken from the compiled tables at some assumed temperature. A check of $\Delta\mu$ from the tables against the $\Delta\mu$ calculated using equation (3) and the values of y_{Ki}, would indicate whether the correct temperature had been chosen. The calculations would have to be repeated until agreement was obtained.

For this approach to be successful, values of C_{Ki} must be obtained from potential models which accurately represent a gas molecule in a hydrate cavity. The Lennard-Jones and Devonshire potentials are restricted in their application and do not adequately represent the majority of gas molecules in the hydrate crystal structure. Other potential models

are available which approximate the physical situation more closely and their application may be successful. Since the success or failure of this method depends almost entirely upon obtaining accurate values of C_{Ki}, a certain amount of calculation and experimental work will be required before this method becomes of practical use.

Following the determination of an adequate potential model, $\Delta\mu$ must be calculated for each structure using the values of C_{Ki} and equation (3b) for a molecular species which will enter only the larger cavity. If the restriction of non-distortion of the crystal lattice by the solute molecules is obeyed, $\Delta\mu$ is independent of the molecular species and depends only upon the fraction of cavities filled. Therefore, only one determination of $\Delta\mu$ is required for each structure. However, there are some molecules such as ethylene which do distort the crystal structure and more experimental work is needed to determine the effect of this distortion.

Two molecular species are required for the calculation of $\Delta\mu$, one for Structure I and another for Structure II. In each case, a molecule should be chosen so that the potential model would closely approximate the physical situation. Sulfur

hexafluoride would probably be the best choice for Structure II due to its spherical molecular structure while bromine could serve for Structure I.

DISCUSSION

A TERNARY SYSTEM SULFUR HEXAFLUORIDE-METHANE-WATER

The stated purpose of this investigation was to test the theory which has been proposed for the gas hydrates. The theory was tested by using it to predict the pressure-composition phase diagram for the sulfur hexafluoride-methane hyrate at -3 degrees Centigrade. From the correspondence between the experimental and predicted diagrams, the theory proposed has been shown to give a very good account of the physical situation. In particular, the form of the equations arising from the theory has withstood the test exceptionally well, indicating that the basic premise is correct, i.e. the occupation of the hydrate cavities may be represented by an idealized Langmuir type equation. Since the Langmuir equations were derived to represent the fraction of active sites on an adsorbing surface which is occupied by adsorbed molecules, the similarity between this situation and the occupation of cavities in a crystal lattice is quite strong. In both cases, at any one temperature, the amount of material which is adsorbed

onto the surface or occupies the different cavities depends only upon the partial pressure and some constant for each molecular species involved. This fact is the major link between the two phenomena. One difference between the two types of phenomena is the fact that adsorption is two-dimensional while gas hydrates are three-dimensional, i.e. the cavities occupy three dimensions. Also, whereas the adsorbed molecules are held onto the active sites by forces comparable to chemical bonding, the hydrated molecules are physically restrained by the surrounding water molecules forming the crystal structure. These differences are not important since they govern only the mechanism by which the host retains the guest mole and the location of the guest molecule. The basic similarity between the two situations is unchanged.

Sulfur hexafluoride was chosen to be studied because it is an almost spherical molecule and because it can occupy only the larger cavity of Structure II. Since both the cavity and the molecule are nearly spherical, the Lennard-Jones and Devonshire potential should give a better description of the molecule in the cavity than for any other molecular species. For this reason, then, the prediction of the pressure-temperature phase diagram should be the best possible

with the Lennard-Jones and Devonshire potential model. The agreement between theory and experiment was not perfect and the deviations which occurred may be due to the approximations arising from the potential model or from limitations in the experimental procedure. Also, the physical data on each of the molecular species involved contains some measure of error. For these reasons, attributing the major cause of the deviation to the potential model, to experiment, or to the physical data is questionable since probably all three contribute appreciably to the resulting deviation.

B RELATIVE STABILITY OF HYDRATE STRUCTURES

In a previous section it was mentioned that the Structure I hydrate appeared to form in preference to that of Structure II and the only time that the latter structure would occur was in systems where the hydrate former was too large to fit into the cavities of Structure I. A thermodynamic justification of this result is now possible from the values of $\Delta\mu^{II}$ calculated in this work for the Structure II hydrate and from the value of $\Delta\mu^{I}$ which has been calculated from the composition of the bromine hydrate determined by Miss Mulders (19). The value of $\Delta\mu$, defined by equation (9),

is the difference between the chemical potential of the water in the hydrate lattice and in the normal states. If a molecular species can exist in two different forms, then from basic thermodynamics the form with the lowest chemical potential will be the most stable. Since the values of $\Delta\mu$ are positive in both cases then the "empty" hydrate lattice is metastable compared with the normal states of water. If the difference between the chemical potential of water in Structure I and in Structure II is defined as $\Delta(\Delta\mu)$, then by the same reasoning it followes that if $\Delta(\Delta\mu)$ is negative, Structure I is stable relative to Structure II.

For Structure I, the values of $\Delta\mu^{I}$ was calculated to be 167 calories per gram mole of water using 8.47 moles of water per mole of bromine as the composition of the bromine hydrate at zero degrees Centigrade. Miss Mulders (19) determined this value using the technique of Scheffer and Meyer (c.f. Theory, section C(3)) and the pressure-temperature phase diagram for the bromine hydrate. She reported the composition to be accurate to plus or minus 0.05 moles of water per mole of bromine and, using the possible limiting values of n, i.e. 8.42 and 8.52, $\Delta\mu^{I}$ was determined to be accurate to plus or minus 2.5 %.

In this investigation, the value of $\Delta\mu^{II}$ was determined by two different methods, one semi-theoretical and the other experimental. The semi-theoretical approach yielded a value of 190 calories per gram mole of water at -3 degrees Centigrade (c.f. Experimental Results, section B) and 192 calories per gram mole at zero degrees. Because the value of C_2 for sulfur hexafluoride is so large, the value of $\Delta\mu^{II}$ is quite insensitive to C_2. For example, a 50% error in C_2 will cause only a 12% error in $\Delta\mu^{II}$.

The experimental value of $\Delta\mu^{II}$ determined in this investigation (c.f. Experimental Results, section A) was 211 calories per gram mole of water. The reliability of this value is open to question because it depends upon the factor $(1 - 17/n)$. Since the ratio of $17/n$ is very close to 1.0, the possible error in n (estimated at plus or minus 0.1) which resulted from the inaccuracies in the experimental data can cause very large errors in $\Delta\mu^{II}$. As n approaches 17, the factor $(1 - 17/n)$ goes to zero and the value of $\Delta\mu^{II}$ approaches infinity. Because the lower limit of n is below 17, a calculation of the upper limit on the accuracy of $\Delta\mu^{II}$ is impossible. The lower limit was calculated to be -25% of the value of $\Delta\mu^{II}$.

[illegible]

[illegible]

[illegible]

Even though the possible errors in n can cause large errors in $\Delta\mu^{II}$ calculated from the experimental data, the agreement between the experimental and semi-theoretical values is satisfactory. The reliability of the value of $\Delta\mu^{II}$ is further enhanced by the good agreement between the experimental and predicted pressure-composition phase diagram for the system sulfur hexafluoride-methane-water.

From the value of $\Delta\mu^{I}$ and the values of $\Delta\mu^{II}$ from the experimental and semi-theoretical methods, $\Delta(\Delta\mu)$ was determined to be -44 and -25 calories per gram mole of water respectively. Using the criterion for relative stability previously mentioned, it follows that Structure I is more stable than Structure II and would tend to be the preferential hydrate structure to form.

CONCLUSIONS

1. The pressure-temperature phase diagram for the system sulfur hexafluoride-water was determined from -8.14 to 12.84°C.

2. The pressure-composition phase diagram was determined on a water-free basis for the system sulfur hexafluoride-methane-water at -3°C.

3. The moles of water associated with each mole of sulfur hexafluoride in the hydrate at 0°C is 17.02 ± 0.1.

4. At 0°C, the heat of formation of sulfur hexafluoride hydrate from ice is -5, 137 calories per gram mole and from liquid water it is -29,568 calories per gram mole.

5. The value of $\Delta\mu^{II}$ calculated at 0°C from experimental data for sulfur hexafluoride is 211 calories per gram mole of water. This compares with 192 calories per gram mole of water calculated from the semi-theoretical approach and with the value of 167 calories per gram mole reported for the $\Delta\mu^{I}$ of Structure I.

6. The statistical mechanical theory proposed for gas hydrates has been shown to adequately describe the thermo-

dynamic behavior of the sulfur hexafluoride hydrate at -3°C.

7. The concept and use of equilibrium constants in hydrate systems has limited theoretical justification and a method of predicting initial hydrate forming conditions based on statistical mechanical theory is required.

AREAS FOR FUTURE INVESTIGATION

1. Equilibrium constants for methane in a hydrate system which crystallizes in Structure I should be investigated in order that these values can be compared with the equilibrium constants for methane when in a system which crystallizes in Structure II. The comparison may yield some information on the effect of cavity geometry on equilibrium constants.

2. Different potential models describing a solute molecule in a hydrate cavity should be applied to gas hydrate systems in order that a model which is adequate for most solutes can be determined.

3. The constants which result from statistical mechanical theory and describe the different solute molecules in a hydrate crystal must be compiled for the various hydrate formers in order that initial hydrate forming conditions may be predicted for any hydrate system.

NOMENCLATURE

c - number of components in the system

C_p - heat capacity at constant pressure

C_{Ji} - a constant characterizing a type J molecule in a type i cavity

f - number of degrees of freedom

F - free energy

G - a gas

h - enthalpy

h_{Ji} - cell partition function for a type J molecule in a type i cavity

H - a hydrate

H_I - a hydrate of Structure I

H_{II} - a hydrate of Structure II

i - type of cavity

I - ice

J - a molecular species

k - Boltzmann's constant

K - equilibrium constant

L_1 - a non-aqueous liquid

L_2 - an aqueous liquid

L_J - absolute activity of the Jth solute molecule

n - number of molecules of water associated with one molecule of hydrate former

N_Q - the total number of Q molecules in the ensemble

N - number of moles in the vapor phase

p_J - the partial pressure of a type J component

p - number of co-existing phases

P - total pressure

q - solubility of gas in water

Q - a molecular species which forms a crystal lattice with cavities into which other molecules can enter

r - moles of water required to saturate the gas phase

r - average atomic distance from an oxygen atom to the centre of the cavity

R - distance from a solute molecule to one of the surrounding molecules

s - quantity of gas dissolved in water

T - absolute temperature

t - temperature in degrees Centigrade

v - number of cavities per molecule of host lattice

V - volume

x - mole fraction in the gas phase

X - potential between a solute molecule and one of the surrounding molecules

y_{Ji} - fraction of type i cavities that are filled with type J molecules

y' - mole fraction of a hydrate former in the hydrate on a water-free basis

Y - mole fraction of a hydrate former in the hydrate

z - number of oxygen atoms surrounding a cavity

exp. - exponential

P.F. - grand partition function

α - the alpha configuration of Q

β - the beta configuration of Q

ε - energy parameter for molecular interaction

σ - distance parameter for molecular interaction

θ_J - molecular partition function of a type J molecule with the volume factor removed

μ - chemical potential

Π - the pi product

Note: In the text both Naperian and Briggsian logarithms are used with the following notation:

log - logarithms to base 10

ln - natural logarithms

BIBLIOGRAPHY

1. Carson, D.B., D.L. Katz, Trans. AIME, 146, 150 (1942)
2. Claussen, W.F., J. Chem. Phys., 19, 1425 (1951)
3. Clegg, H.P., I.S. Rowlinson, R.J. Sutton, Trans. Faraday Soc., 51, 1327 (1955)
4. Dale, M., "Introduction to Statistical Thermodynamics" Chapter 9, Prentice-Hall, Inc. (1960)
5. Evans, D.F., R.E. Richards, Proc. Roy. Soc. (London) A 223, 238 (1954)
6. Faraday, M., Phil. Trans., 22, 160 (1823)
7. Forcrand, R. de, compt. rend., 94, 967 (1882)
8. Forcrand, R. de, P. Villard, compt. rend., 106, 849, 939, 1357, 1402 (1888)
9. Fowler, R.H., E.A. Guggenheim, "Statistical Thermodynamics" University Press, Cambridge (1952)
10. Friedman, H.L., J. Am. Chem. Soc., 76, 3294 (1954)
11. Gambill, W.R., Chem. Eng., 64, 243 (June 1957)
12. Hammerschmidt, E.G., Ind. Eng. Chem., 26, 851 (1934)
13. Hammond, S.D., J.A. Lambert, R.B. Thomas, Australian J. of Chem., 8, 49 (1955)
14. Isambart, R.J., compt. rend., 86, 481 (1878)
15. Katz, D.L., et al, "Handbook of Natural Gas Engineering", McGraw-Hill (1959)

16. Lennard-Jones, J.E., A.F. Devonshire, Proc. Roy. Soc. (London), A163, 53 (1937); A165, (1938)

17. Matheson of Canada, Ltd., Private Communication, (1961)

18. Mueller, W.H., T.W. Leland, R. Kobayashi, A.I.Ch.E. J., 7, 267 (June 1961)

19. Mulders, E.M.J., Thesis, Delft, (1937)

20. Nikitin, B.A., Bull. Acad. Sci. (U.S.S.R.), 1, 39 (1940) Chem. Abst., 35, 3494 (1941)

21. Otto, F., M.Sc. Thesis, Alberta (1959)

22. Palin, D.E., H.M. Powell, Nature 156, 334 (1945); J. Chem.Soc. (London), 208 (1947); 571 (1948)

23. Powell, H.M., rec. trav. chim., 75, 855 (1956)

24. Platteeuw, J.C., J.H. van der Waals, rec. trav. chim., 78, 126 (1959)

25. Reamer, H.H., F.T. Selleck, B.H. Sage, Trans. Am. Inst. Min. & Met. Engrs., 195, Tech. Pub. No. 3376; J. Pet. Tech., 9, No. 8, 197 (1952)

26. Scheffer, F.E.C., G. Meyer, vers. akad. wetenscheppen (Amsterdam), 21, 1104 (1919)

27. Snell, L.E., M.Sc. Thesis, Alberta, (1960)

28. Stackelberg, M. von, Naturwiss, 36, 327, 359 (1949)

29. Stackelberg, M. von, H.R. Muller, Z. Elektrochem., 58, 25 (1954)

30. Stackelberg, M. von, W. Meinhold, Z. Elektrochem., 58, 40 (1954)

31. Stackelberg, M. von, H. Fruhbuss, Z. Elektrochem., 58, 99 (1954)

32. Villard, P., compt. rend., 106, 1602 (1888)

33. Waals, J.H. van der, J.C. Platteeuw, "Clathrate Solutions", Advances in Chemical Physics, Vol. II (1960)

34. Waals, J.H. van der, Trans. Faraday Soc., 52, 184 (1956)

35. Wilcox, W.I., D.B. Carson, D.L. Katz, Ind. Eng. Chem., 33, 662 (1941)

Note: The references published before 1900 were obtained from the following source:

Katz, D.L., M.J. Rzaza, "Bibliography for Physical Behavior of Hydrocarbons Under Pressure and Related Phenomena", J.W. Edwards, Inc., 244-249 (1946)

APPENDIX

- A -

THE METASTABLE EQUILIBRIUM OF HYDRATE-GAS-ETHYLENE GLYCOL SOLUTION

Hydrates will exist while in equilibrium with gas and a water-ethylene glycol solution. The effect of the ethylene glycol is to decrease the temperature at which hydrates will form for a given pressure. During the experimental determination below zero degrees Centigrade, sub-cooling was required to initiate ice formation and if hydrate was formed prior to ice formation, a metastable equilibrium was established in which hydrate, gas and water-ethylene glycol solution co-existed. The pressure was lower than the equilibrium pressure between hydrate-gas-ice and as soon as an ice phase appeared, the pressure increased to the equilibrium value for the hydrate-gas-ice system. Diagrammatically this is shown in Figure XIX where the lower part of Figure VII is reproduced with HL_2G lines added for increasing amounts of ethylene glycol. Suppose "t" degrees Centigrade was the temperature under consideration and a glycol solution was prepared so that approximately half would become ice at "t". This solution would contain X% ethylene glycol before ice formation and Y% after-

FIGURE XIX

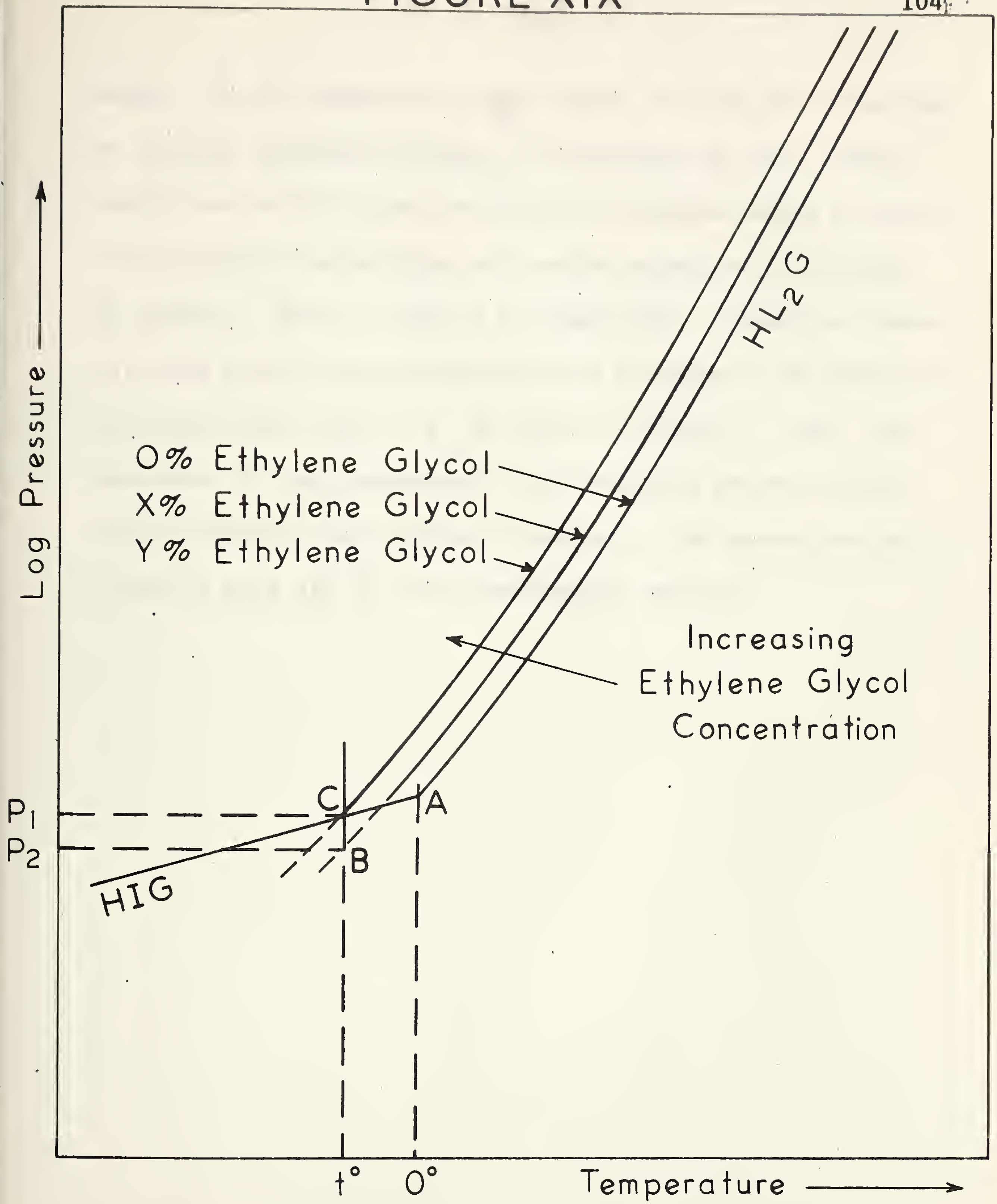

Qualitative Effect of Ethylene Glycol on the Equilibrium $H \cdot L_2G$

wards. If the temperature was set at "t" and the formation of hydrate initiated without the presence of ice, hydrate would form until P_2 was reached, the hydrate being in equilibrium with a metastable sub-cooled solution containing X% glycol. This is point B in Figure XIX. Upon ice formation the glycol concentration would increase to Y% and the pressure would rise to P_1 as shown by point C. With the presence of this phenomenon, ice formation prior to that of the hydrate was mandatory leading to the procedure outlined in part (B) of the Experimental section.

- B -

TABULATIONS

TABLE I

EXPERIMENTAL PRESSURE-TEMPERATURE DATA FOR THE SYSTEM SULFUR HEXAFLUORIDE-WATER

Temperature - °C	Pressure - psia
.56	13.1
.66	13.4
1.05	14.4
1.63	15.7
2.19	17.55
2.97	21.1
3.03	21.2
3.73	24.7
4.74	31.5
4.79	31.7
6.05	41.3
6.93	51.3
7.05	51.9
7.87	65.6
9.90	106.8
11.18	144.0
11.51	159.9
11.72	165.2
12.84	219.0
- .26	11.68
- .64	11.78
-1.06	11.38
-1.31	11.16
-1.96	11.12
-2.51	10.78
-3.16	10.40
-3.81	10.41
-4.29	9.72
-4.91	9.46
-5.00	9.62
-5.67	9.20
-6.57	8.66
-7.50	7.97
-8.14	7.90

TABLE II

EXPERIMENTAL PRESSURE-COMPOSITION DATA FOR THE SYSTEM SULFUR HEXAFLUORIDE-METHANE-WATER AT -3°C

Total Pressure		Mole Per Cent SF_6 on a Water-Free Basis	
psia	Atmospheres	In the Hydrate	In Gas Phase
10.52	.716	100.0	100.0
13.5	.92	89.6	70.3
19.7	1.34	75.1	41.8
23.1	1.57	69.6	27.6
28.8	1.96	66.5	21.5
49.6	3.38	60.8	10.5
58.2	3.96	54.4	7.0
85.0	5.78	43.4	2.8
116.9	7.95	42.2	1.5
159.8	10.87	37.1	0.6
248.4	16.90	27.0	0.5
342.1	23.28	0.0	0.0

TABLE III

DATA FROM THE THEORETICAL PREDICTION OF THE PRESSURE-COMPOSITION PHASE DIAGRAM FOR THE SYSTEM SULFUR HEXAFLUORIDE-METHANE-WATER AT -3°C

Total Pressure		Mole Per Cent SF_6 on a Water-Free Basis	
psia	Atmospheres	In the Hydrate	In Gas Phase
11.3	.77	96.9	90.0
12.3	.84	93.6	80.0
13.5	.92	90.1	70.0
14.8	1.01	86.3	60.0
16.8	1.14	82.2	50.0
19.3	1.31	77.6	40.0
23.1	1.57	72.5	30.0
29.4	2.00	66.2	20.0
43.1	2.93	57.9	10.0
61.4	4.18	51.8	5.0
94.3	6.42	45.7	2.0
127.1	8.65	42.0	1.0
167.7	11.41	38.6	0.5
220.4	15.00	34.5	0.23
288.9	19.66	28.6	0.1
307.3	20.91	26.8	0.08
330.7	22.50	24.3	0.06
362.1	24.64	20.5	0.04
408.3	27.78	14.1	0.02
441.5	30.04	8.7	0.01
482.2	32.81	1.1	0.001
488.	33.2	0.0	0.0

TABLE IV

EQUATIONS FROM THE LEAST SQUARE CURVE FIT OF THE EXPERIMENTAL PRESSURE-TEMPERATURE DATA FOR THE SULFUR HEXAFLUORIDE-WATER SYSTEM

Above 0°C

$$\ln P = 2.4701 + 0.17365\, t + 7.2349 \cdot 10^{-3}\, t^2 - 2.3908 \cdot 10^{-4}\, t^3$$

Standard Deviation of Points - 0.86 psia

Standard Deviation of Curve - 0.20 psia

Below 0°C

$$\ln P = 2.4720 + 3.1262 \cdot 10^{-2}\, t + 2.5046 \cdot 10^{-3}\, t^2$$

Standard Deviation of Points - 0.14 psia

Standard Deviation of Curve - 0.035 psia

Equations for Standard Deviations

Standard Deviation of Points = $(d^2/(n-m))^{1/2}$

Standard Deviation of Curve = $(d^2/n(n-m))^{1/2}$

Where:

d - the difference in pressure between the data and the curve at the temperature in question

n - the number of experimental points

m - the order of the equation to which the data is being fitted

TABLE V

EQUATIONS FOR THE WEIGHTED LEAST SQUARE CURVE FIT OF A LINEAR CURVE

Nomenclature

x_i, y_i - coordinates of an experimental point

x, y, - coordinates of a point on the fitted curve corresponding to the experimental point (x_i, y_i)

D - the distance between y and y_i

n - number of experimental points

Initial Equations

$$D = y_i - (a\,x + b)$$

$$y = a\,x + b$$

Restrictions

The values of the two variables, x_i and y_i, are both in error and the relation joining the experimental point (x_i, y_i) with the corresponding point (x, y) on the fitted curve is:

$$(y - y_i)/(x - x_i) = \tan \theta$$

where θ is the angle between the line joining the point (x_i, y_i) to (x, y) and the absicissa of the coordinate system. This angle is usally a constant for each curve fit.

TABLE V (cont'd)

Criterion for Least Squares

$$\frac{\partial}{\partial a} \sum D^2 = 0$$

$$\frac{\partial}{\partial b} \sum D^2 = 0$$

Resulting Expressions for the Coefficients of the Linear Equation

$$a = A/B$$

$$A = \tan\theta \sum x_i y_i - \tan\theta \left(\sum x_i \sum y_i\right)/n + \left(\sum y_i\right)^2/n - \sum y_i^2$$

$$B = \tan\theta \sum x_i^2 - \tan\theta \left(\sum x_i\right)^2/n + \sum x_i \sum y_i/n - \sum x_i y_i$$

$$b = \left(\sum y_i - a \sum x_i\right)/n$$

TABLE VI

CALCULATION OF THE HEAT OF FORMATION OF THE SF_6 HYDRATE AT 0°C

Heat Capacities, Calories per Gram Mole per °C

H_2O (liquid, 0°C) - 18.15

H_2O (solid, 0°C) - 9.11

SF_6 (gas, 25°C) - 23.22 (ref. 17)

SF_6 (solid) - 35.4 (estimated by Kopp's Rule and data from Gambill (11))

SF_6 Hydrate - 141 (estimated by Kopp's Rule and assuming 17 water molecules per molecule of SF_6)

Corrections to Δh Calculated from Equation (28)

Correction - Calories	t 0°C	t 0°C
To 0°C (equation (29))	253.8	17.1
Evaporation of Water (equation (24))	81.3	92.2
Solubility of SF_6 in Water (ref. (10)) (equation (25))	-1.1	0.0
TOTAL	334.0	109.3

TABLE VI (cont'd)

The Δh from Equation (28)

$-\Delta h/NR$ = slope of the plot of the left hand side of equation (28) against $1/T$

R = 1.9872 calories per gram mole per degree Kelvin

N = from equation (26)

Data and Calculated Results

Item	t 0°C	t 0°C
Temperature at the mid-point of the interval	1.86	-1.90
N	-1.00740	-1.00757
Slope from equation (28)	-6487.2	-1138.0
Δh	-29,903.3	-5246.3
Δh (0°C corrected)	-29,569.3	-5,137.0
$\Delta(\Delta h)$	24,432.3	
$\Delta h_{\text{fusion of ice}}$	1,435.2	
n (equation (33))	17.023	
$\Delta\mu^{II}$ (equation (3b))	211.2	

Note: The units of enthalpy are calories per gram mole of SF_6 in the hydrate and the units of chemical potential are calories per gram mole of water.

- C -

EQUIPMENT CALIBRATIONS

FIGURE XX

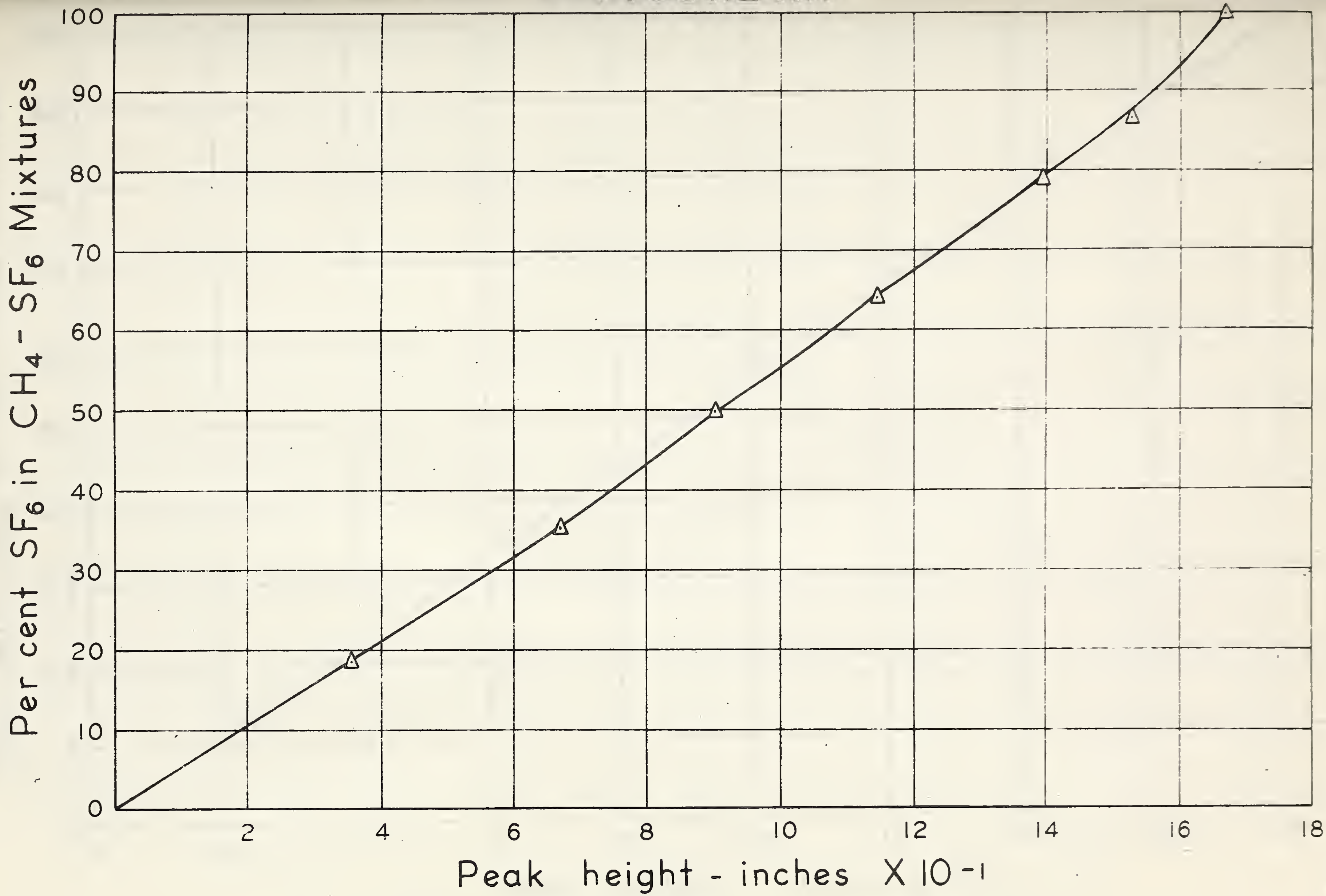

Kromo-Tog Calibration for SF6

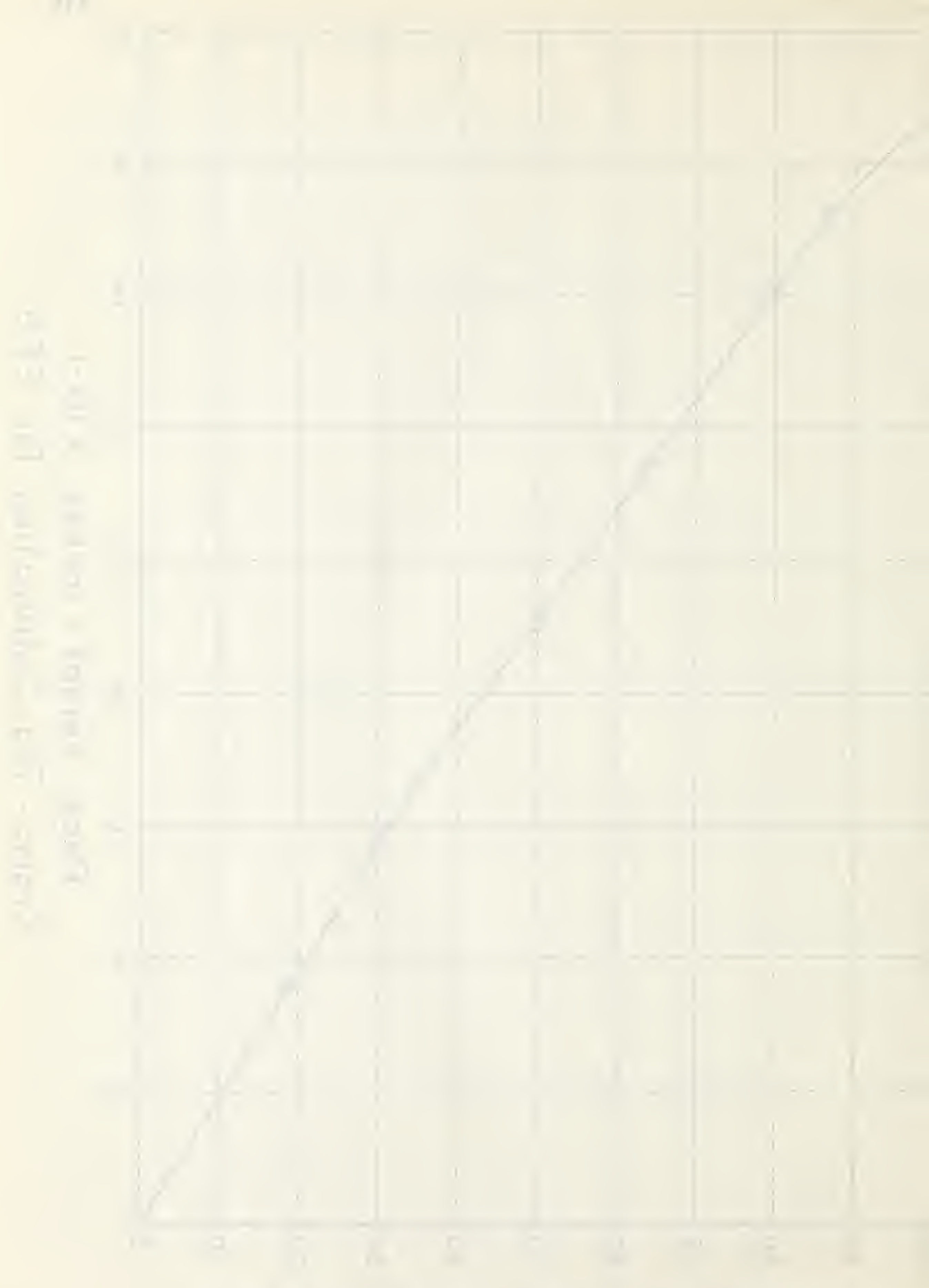

FIGURE XXI

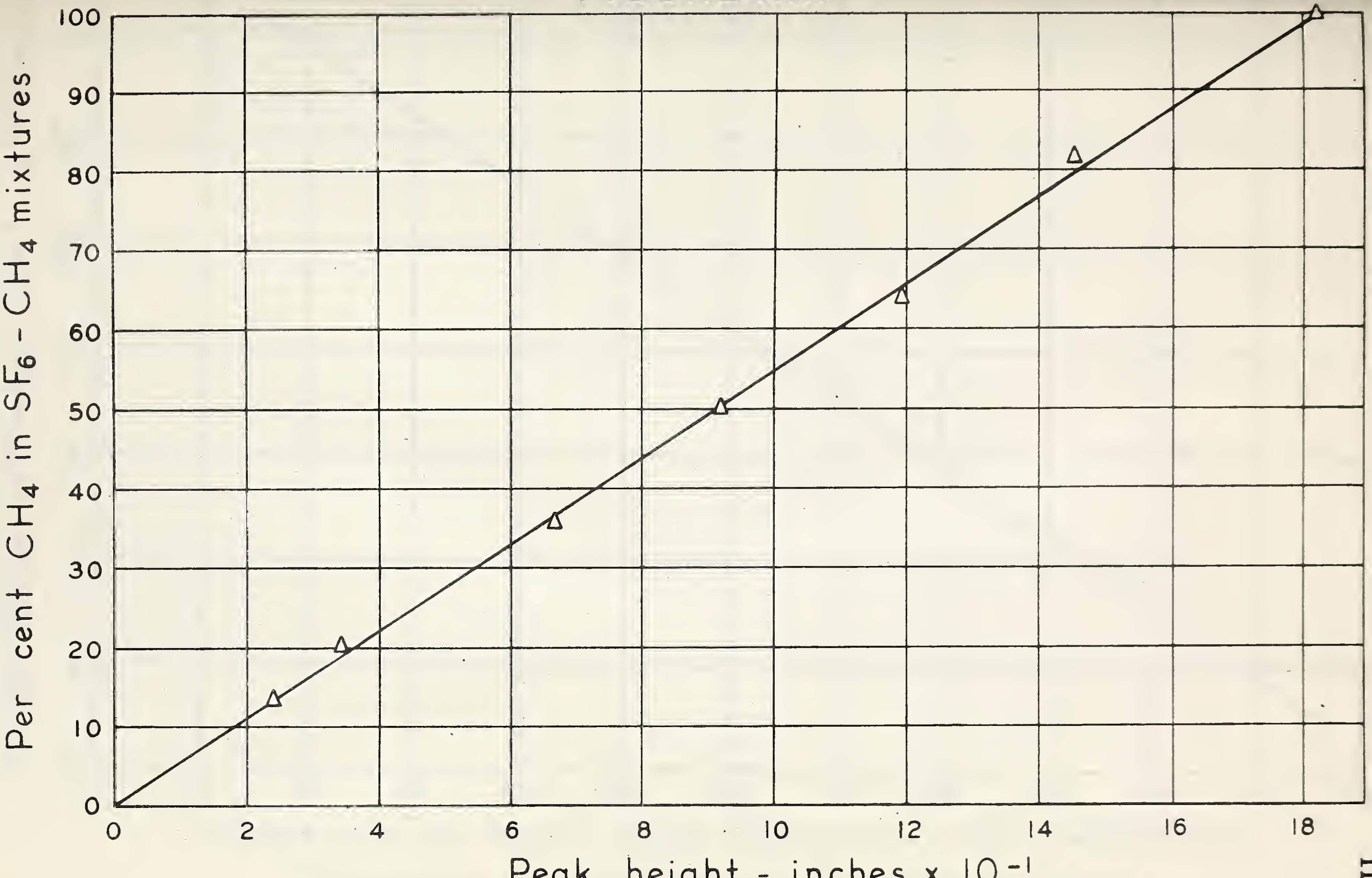

Kromo - Tog Calibration for CH_4

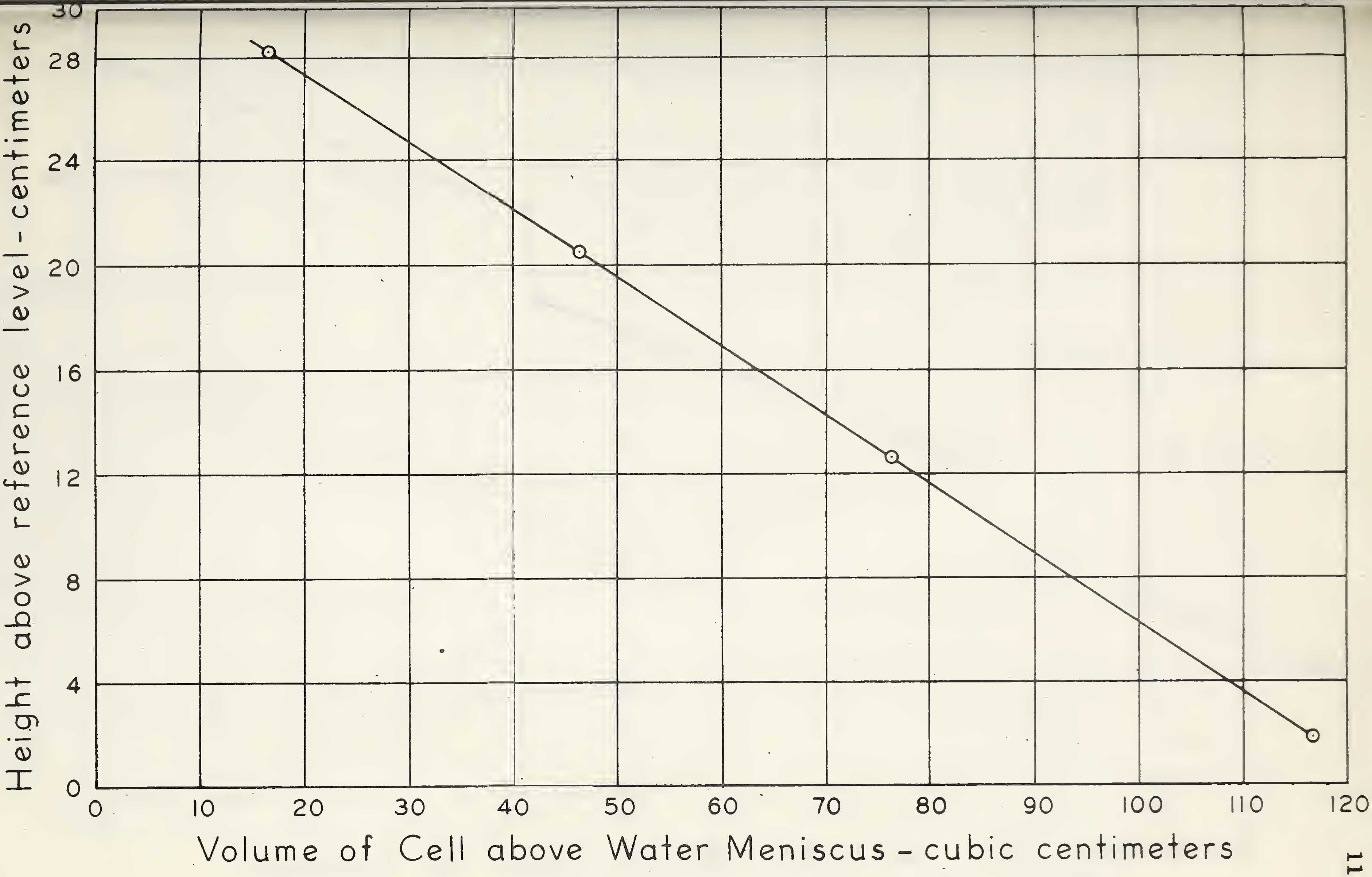

Volumetric Calibration of Equilibrium Cell

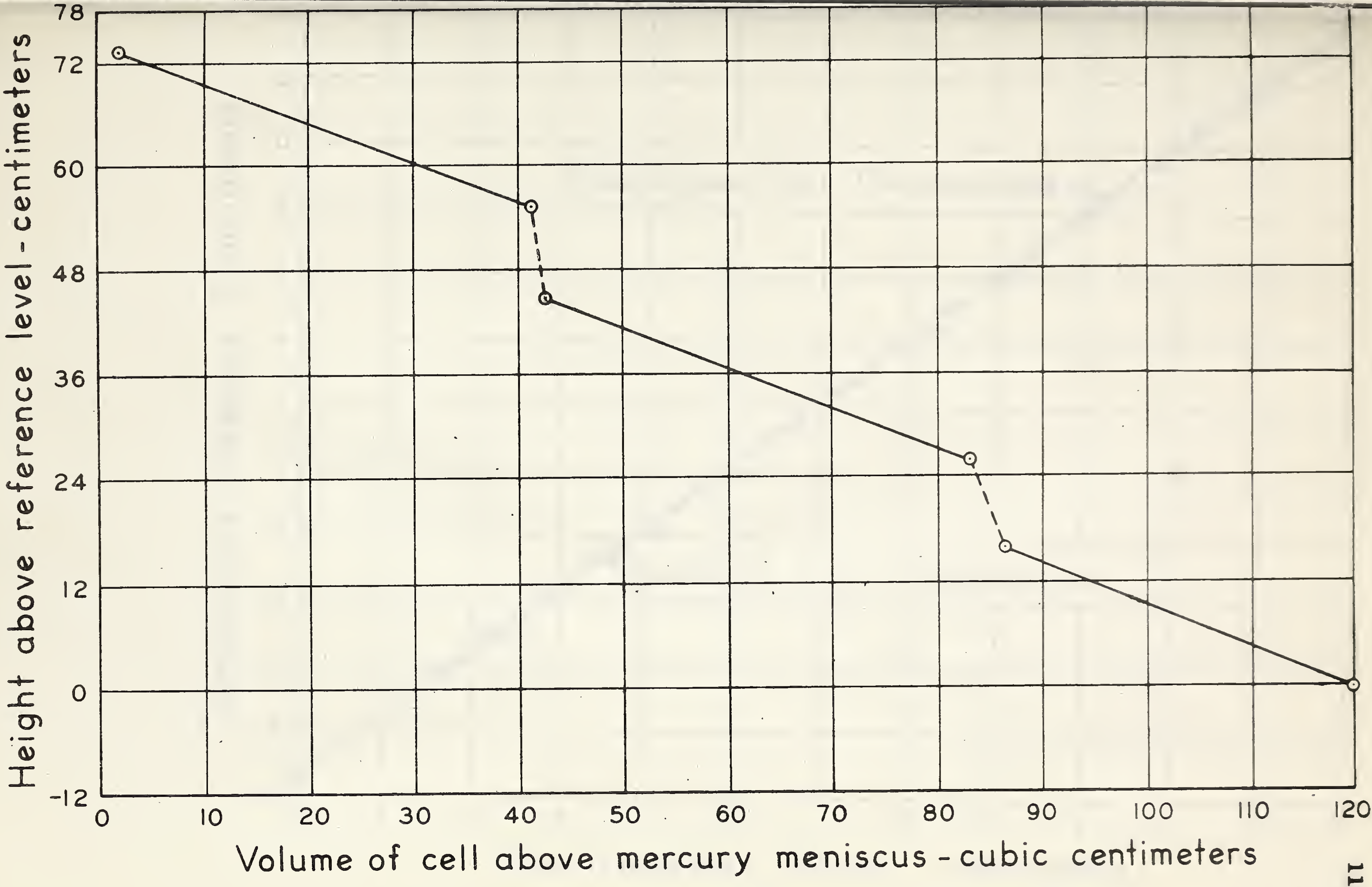

Volumetric Calibration of Auxiliary Cell

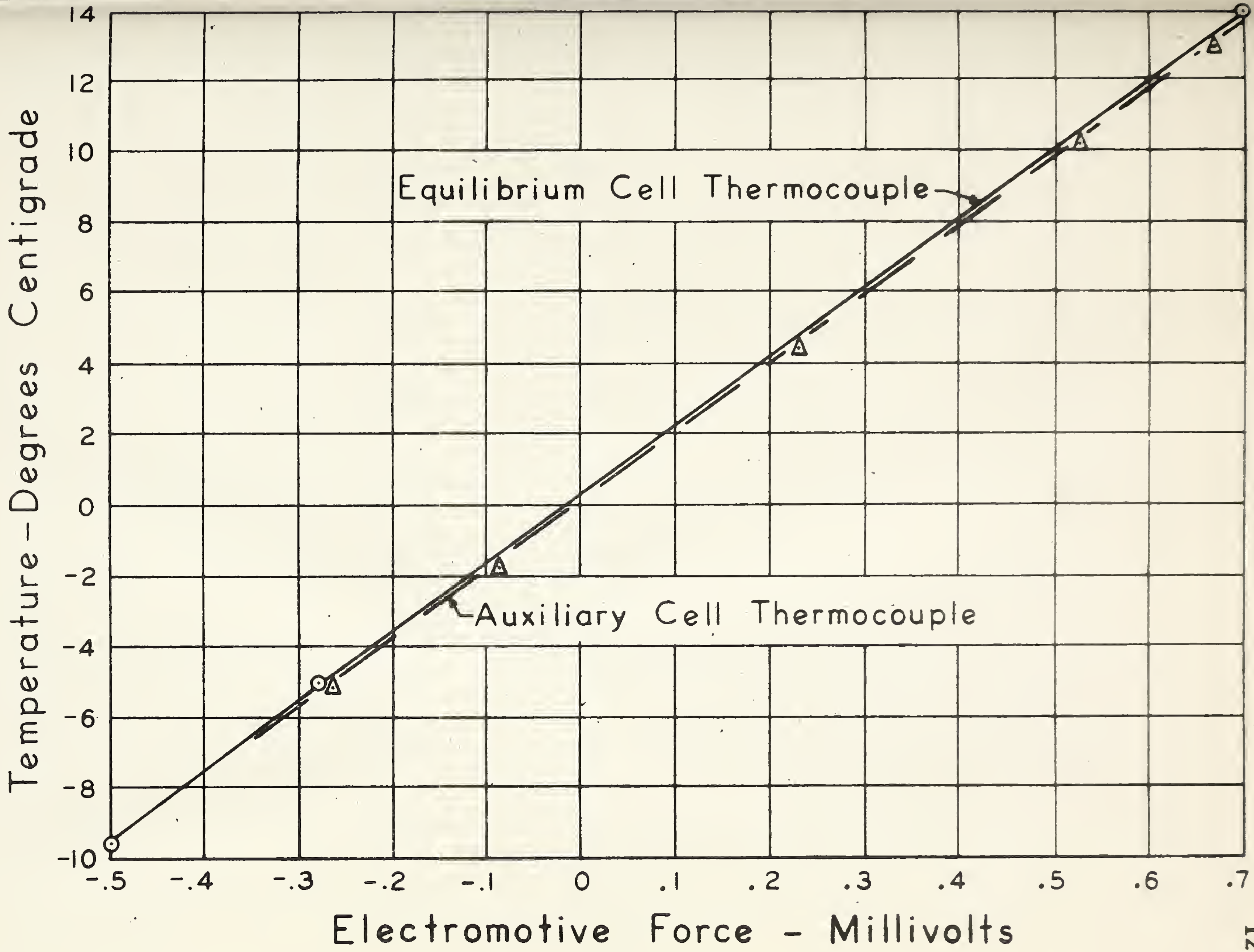

Iron-Constantan Thermocouple Calibration

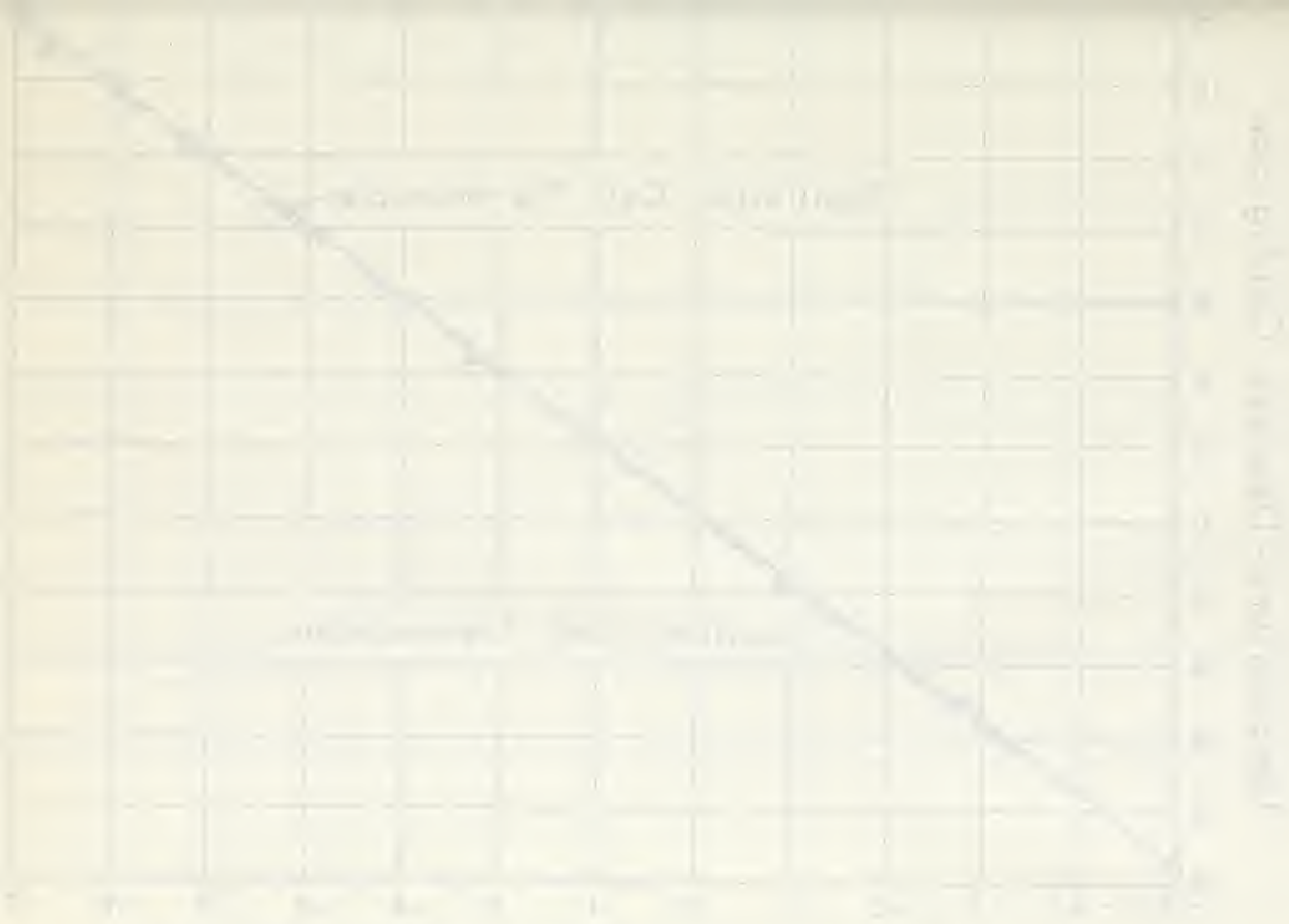

[illegible] Thermocouple Calibration

B29798